**Nd Isotopic, petrologic and geochemical investigation of the Tulawaka East gold deposit, Tanzanian shield.**

!

!

!

!

!

[1]*Cloutier, Jonathan;*

[1]*Stevenson, Ross K.;*

[1]*Bardoux, Marc*.!

!

!

!

!

!

!

!

!

!

!

[1]*GEOTOP et Département des Sciences de la Terre et de l'Atmosphère, Université du Québec à Montréal, P.O. Box 8888, Succ. Centre-ville, Montréal, Québec, H3C 3P8*

**Abstract**

New isotopic (Sm-Nd) and geochemical data are presented for volcano-sedimentary and granitic lithologies of the Tulawaka East gold deposit in the Late Archean Sukumaland greenstone belt of the Tanzanian Shield. The data help to characterize the geological environment of the greenstone belt/gold deposit and the crustal evolution of the Tanzanian Shield. The volcano-sedimentary units are intruded by leucogranites and aplitic dykes that were deformed and metamorphosed to amphibolite facies. The Au mineralization occurs in thrust faults at the contact between the aplite dykes and the volcano-sedimentary units. The metavolcanic rocks are largely basaltic to intermediate in composition with negative Nb anomalies and flat Rare Earth element (REE) profiles varying from 10 to 100x chondritic values. Initial $\varepsilon Nd_{2.8\ Ga}$ values vary from +0.9 to +5.3 and Nd model ages ($T_{dm}$) range from 2.8-3.0 Ga. The metasedimentary rocks are generally enriched in light REE (100x chondrite) with weak negative Eu anomalies and $\varepsilon Nd_{2.8\ Ga}$ values vary from 0.0 to +2.6. The leucogranites are garnet-rich and peraluminous with strong negative anomalies in Eu and Ti and with flat REE profiles (10-100x chondrite). The aplite dyke is also peraluminous with similar negative Eu and Ti anomalies and a flat light REE, but is depleted in heavy REE. The similarity in composition with the leucogranite suggests that the two are cogenetic and formed by fractionation of a more mafic parent. The combination of the flat REE element patterns and negative Nb anomalies among the mafic volcanic rocks suggests formation as an immature (island?) arc at ca. 2.8 Ga. However, Nd isotope signatures in the metasedimentary rocks provide evidence of an older crustal sedimentary provenance (ca. 3.0-3.1 Ga) and proximity of a continental influence. The age of the leucogranite and aplite dyke are constrained by a Sm-Nd garnet-whole-rock age of ca 2.5 Ga, indicating that the shear zone-hosted gold mineralization is younger than 2.5 Ga. The range of isotopic compositions found in the Tanzanian Shield overlap with those of the Zimbabwe Craton to the south.

## Introduction

The African continent consists of some 13 Archean cratons (Goldfarb et al., 2001) that, in addition to representing important mineral exploration targets, are crucial to understanding the geological evolution of the African continent. The Tanzanian Shield is the fourth largest of these cratons and endowed with diamonds, nickel, cobalt and copper (Yager, 2000), as well as being one of the most attractive targets for gold exploration in the past decade (Tassel, 2003). This gold is found mainly within the Archean Sukumaland greenstone belts and iron formation of the Lake Victoria goldfields district including the Bulyanhulu and Geita gold mines.

Tulawaka East is a new gold deposit located in southwestern Sukumaland, 100 km west of the Bulyanhulu mine and 700 km northwest of the capital city of Dar es Salaam (Fig. 1 and 2). The Tulawaka East gold deposit is one of several gold occurrences on the Tulawaka property discovered in 1997 by Pangea Goldfields ltd. through geochemical anomalies. Major and trace element data and Sm-Nd isotopic data are presented for supracrustal and granitoid samples from the Tulawaka East Gold deposit in order to characterize the source and age of gold mineralization, and place constraints on the geological environment of the deposit and implications for the evolution of the Tanzanian Craton. The growth of Archean cratons represents an important period in Earth history for crustal stabilization and/or crustal growth (e.g. Albarède, 1998; Stevenson and Patchett 1990; Condi, 1989; Patchett and Arndt, 1986; Taylor and McLennan, 1985) and a better understanding of the evolution of the Tanzanian Craton would benefit both African and global crustal evolution/tectonic models.

## Geology

The Tanzanian shield is bordered by, and in tectonic contact, with three Proterozoic mobile belts: the Ubendian, the Usagaran and the Mozambique belts (Ring, 1993; Lenoir et al.,

1994). The Tanzanian Shield is divided between the Dodoman Group (and Dodoman Belt) of granites, granodiorites, granitic gneisses, migmatites and high-grade metamorphic supracrustal rocks that cover the central portion of Tanzania and the Nyanzian Supergroup of granite-greenstone belts that are found mainly in the north and west (Figure 1; Clifford, 1970; Wade and Oates, 1938). The Nyanzian Supergroup is sub-divided between the Lower Nyanzian and the Upper Nyanzian. The Lower Nyanzian is traditionally considered to be the lowermost part of the greenstone belt succession and is composed primarily of tholeiitic amphibolites and metagabbros with minor occurrences of meta-andesites and ultramafic rocks while the Upper Nyanzian forms the uppermost part of the greenstone belt and is composed of chemical (iron formation) and clastic sedimentary rocks and metavolcanic rocks that are mainly rhyolitic in composition (Borg and Shackleton, 1997; Borg, 1992).

One of the larger greenstone belts of the Tanzanian Shield is the Sukumaland greenstone belt which is an oval shaped belt (Fig. 1 and 2) defined by two intermittently exposed belts of metavolcanic and metasedimentary rocks that surround a core of granitoids and gneisses (Borg and Krogh, 1999). The geology of the belt consists mainly of Archean volcano-sedimentary sequences of the Nyanzian Supergroup (2.6-2.8 Ga). The Rwamagaza/Ushirombo inner belt comprises mafic (tholeiitic amphibolite and metagabbro) and minor intermediate (andesites) metavolcanic sequences of the Lower Nyanzian (Kuehn et al., 1990; Borg and Krogh, 1999) while the Geita outer belt consists of banded iron formation and clastic metasedimentary rocks and felsic and intermediate metavolcanic sequences (mainly rhyolites) of the Upper Nyanzian (Barth 1987; Borg and Krogh 1999). As a whole, the belt is dominated by mafic volcanic rocks (basalt-andesite 70%), with lesser amounts of felsic (20%) and metasedimentary (10%) units (Borg and Shackelton, 1997). Manya (2001) suggested that the greenstone belt units formed in an arc/back-arc setting. These units were subsequently metamorphosed to greenschist and locally to

amphibolite facies and then intruded by Archean granites and granodiorites of Archean age (Bell and Dodson, 1981).

A Sm-Nd age of 2823±44 Ma for a meta-basalt from the Lower Nyanzian (Manya and Maboko, 2003) and U-Pb zircons ages of 2780±3 and 2808±3 and 2699±9 Ma for felsic pyroclastic rocks of the Upper Nyanzian in the Bulyanhulu and Geita mines areas (Borg and Krogh, 1999) suggest a more complex relationship than that implied by a younger Upper and older Lower Nyanzian. A 2680±3 Ma age for migmatitic gneisses in the Geita area also raises questions about the traditional view that the Dodoman Group constitutes the basement to the Nyanzian greenstone belts (Borg et al., 1990; Borg and Krogh, 1999).

The Tulawaka property (Fig. 2 and 3) lies within the Sukumaland greenstone belt at the western intersection of the inner and the outer belts (Robinson and Aubertin, 2000). At Tulawaka East, the volcano-sedimentary sequences of the Nyanzian Supergroup are metamorphosed to amphibolite facies and are intruded by a leucogranite and by aplitic dykes. The Tulawaka East deposit is one of several gold occurrences on the Tulawaka property. Gold mineralization occurs throughout the Sukumaland belt in various styles as: (1) vein-type and shear zone-hosted, (2) associated with volcanogenic massive sulphide (VMS) and (3) as sulphidic replacement ore in banded iron formation (Kuehn et al., 1990; Borg, 1993). Dating of a lamprophyre dyke that texturally pre-dates gold mineralization in the Geita mine yields a maximum age for gold mineralization of 2644 Ma (Borg and Krogh, 1999). Gold mineralization on the Tulawaka property is shear zone hosted type and is mainly found in detachment zones, near the leucogranite, at the contact between the aplitic dykes and volcano-sedimentary sequences. The age of this mineralization is part of this present study.

**Samples and Methodology**

The surface geology at Tulawaka is obscured by extensive laterite coverage, thus samples studied herein were obtained from drill core (D0142, D0146, D0149, D0159, D0185, D0309 and D0310). D0149 and D0159 consist mainly of metasedimentary rocks, D0146, D0185 and D0309 are mainly metavolcanic rocks and D0310 is a leucogranite. Sample D0142 is a sample of an aplitic dyke hosting the gold mineralization. Typical metamorphic assemblages for the metasedimentary rocks include staurolite, biotite and feldspar with occasional muscovite and chlorite. The typical assemblage for the metavolcanic rocks is hornblende, feldspar and biotite with occasional garnet, muscovite and chlorite. The leucogranites consist of quartz, feldspar, muscovite and garnet (without zircon) while the aplitic dyke consists mainly of feldspar and quartz (Thompson, 2002)

Rock samples for Sm-Nd analyses were cleaned and crushed to a powder in preparation for whole-rock dissolution and chemical separation. A $^{149}Sm$-$^{150}Nd$ tracer was added for determination of Nd and Sm concentrations. All samples were dissolved under pressure in HF-$HNO_3$ mixture in Teflon containers for one week. Rare earth elements (REE) were extracted from the samples by standard elution techniques using HCl on cation-exchange columns. Nd and Sm were separated from REE on orthophosphoric acid-coated Teflon powder after Richard et al. (1976). A full description of the analytical procedures used in the GEOTOP laboratories can be found in Henry et al. (1998).

Nd and Sm isotopic ratios were measured on a VG SECTOR-54 mass spectrometer at l'Université du Québec à Montréal. Mass fractionation was corrected by normalizing $^{146}Nd/^{144}Nd$ to 0.7219. The reference values used in $\varepsilon_{Nd}$ calculations are $^{143}Nd/^{144}Nd_{CHUR}$ = 0.512638, $^{147}Sm/^{144}Nd_{CHUR}$ = 0.1967 and $^{147}Sm = 6.54 \times 10^{-12}\ a^{-1}$. A formation age of 2.8 Ga was used for

the εNd calculation for the metasedimentary rocks and a formation age of 2.5 Ga was used for the leucogranites and aplite sample. The uncertainty in the εNd values is approximately 0.5 εNd units.

The garnet compositions were derived by back-scatter electron analyses using a Hitachi S-2300 Scanning Electron Microscope. Filament voltage was at 20 KV and an Rx detector (Kevex Quantum SeLi detector) was used for low atomic number elements. The SEM has an IXRF computing system with a count time for the RX spectrum of 50 sec at 40 % dead time level. For backscatter electron analyses, a Gini type 113A backscatter was used. Major and minor element whole-rock compositions were analyzed by ICP-MS.

## Results

### *Geochemistry*

The whole rock compositions for samples from the Tulawaka East deposit are presented in Tables 2 and 3 and major elements are plotted in figure 6. The metasedimentary rocks are largely intermediate in composition with average $SiO_2$ and $Al_2O_3$ concentrations of 60 and 20% respectively. There is a decrease in MgO, $TiO_2$, $K_2O$ and $Al_2O_3$ and an increase in CaO with increasing $SiO_2$ among the metasedimentary rocks that may reflect a decrease in clay mineral content and an increase in quartz and feldspar content. The metavolcanic rocks are mainly basalts and andesites with minor amounts of dacites (D0149-3 and D0149-13; Fig. 4). There is a general decrease in MgO, $TiO_2$ and CaO with increasing $SiO_2$ in the metavolcanic rocks which likely reflects differentiation of the basaltic melts. A lack of correlation for K, Ca and Al is probably due to a combination of hydrothermal remobilization of these elements and subsequent overprinting by amphibolite facies metamorphism. There are insufficient leucogranite and aplite

samples to determine any trends, however, the leucogranites are peraluminous (A/CNK = 1.7-2.0; Shand, 1927) and have average $SiO_2$, $Al_2O_3$ and $Na_2O$ contents of 75, 15 and 4.6% respectively.

The chondrite normalized REE profiles are plotted in figure 7. The REE profiles for the metasedimentary rocks show a general enrichment in LREE (average 100x chondrite) with a weak Eu depletion and are somewhat similar to the North American Shale Composite (NASC) profile (Fig. 7a). However, the NASC profile plots in the upper part of the metasedimentary rock field and is enriched in HREE. The mafic metavolcanic rocks are characterized by flat profiles between 10-100 times the chondritic ratio (Fig. 7b), while the felsic metavolcanic rocks are LREE enriched (Fig. 7c). The leucogranites REE profiles are relatively flat between 10-100 times the chondritic ratio with a strong negative Eu anomaly (Fig. 7d). The aplite has a profile similar to that of the leucogranites, but with a strong depletion in HREE (Fig. 7d).

The trace element profiles of metasedimentary rocks are depleted in Nb, Zr and Ti (Fig 8a.) and show a similar trend to the North American Shale Composite (NASC) profile. Once again, however, the NASC profile is more enriched than the average Tulawaka metasedimentary rock with notably strong enrichments in Zr, Hf and HREE. Metavolcanic rocks have flat profiles (10-100x chondrite) with depletion in Nb and Ti similar to the sedimentary rocks profiles (Fig 8b-c). The felsic metavolcanic samples tend to be enriched in Th and more depleted in Nb compared with the mafic metavolcanic rocks. The leucogranites and aplitic dyke exhibit similar profiles with clear Th enrichment and Zr, Eu and Ti depletion except that the aplitic dyke exhibits a deep depletion in HREE (Fig 8d). Leucogranitic samples tend to have depletions in Ba, Sr and Eu suggesting either feldspar fractionation from the melt or residual feldspar in the source.

*Isotope geology*

Table 4 shows the results obtained for 28 whole-rocks and 5 garnet fractions analysed for Sm-Nd isotopes. Whole-rock εNd values are calculated at 2800 Ma, reflecting their possible Lower Nyanzian ages (Borg and Krogh, 1999). The metasedimentary rocks have εNd values ranging between 0.0 and +2.6 with $^{147}Sm/^{144}Nd$ ratios varying from 0.1003 to 0.1204. The metavolcanic rocks have εNd value ranging between +0.9 and +5.3 with $^{147}Sm/^{144}Nd$ ratios between 0.11 and 0.21. The leucogranites have εNd values of –0.7, +3.9 and +5.8 with $^{147}Sm/^{144}Nd$ ratios of 0.23 and 0.20 for the last two. The aplite dyke gives an εNd value of –12.6 with a $^{147}Sm/^{144}Nd$ ratio of 0.4015. Model ages ($T_{dm}$) obtained from metasedimentary and felsic volcanic samples give Archean ages of 2.8-3.0 Ga. The metavolcanic rocks follow the isochron of 2823±44 Ma generated by Manya and Makobo (2003) for metabasalts from the northeastern part of the Sukumaland greenstone belt (Fig. 9) and are thus broadly consistent with an Archean age. Without better field constraints to tell if the volcanic rocks are all from the same event, it is impossible to say if this is a real age or an average age for the entire suite. Nevertheless the Nd model ages indicate that the metasedimentary and the metavolcanic rocks are Archean and were likely formed at about the same time as the volcanic rocks analysed by Manya and Makobo (2003). The metasedimentary samples appear to form a linear array in an isochron diagram (Fig. 9), however, this likely reflects a mixture between different sedimentary sources rather than real age information. This view is corroborated by the correlation between εNd and Nd concentrations (Fig. 10) that indicates that the Nd isotope compositions result from a mixture between a juvenile source (volcanic sediments) and an older source (continent-derived sediments/Dodoman Group?).

Igneous (D0310-1) and metamorphic garnets (D0149-4, D0149-13 and D0149-20) were sorted for Sm-Nd analyses. The igneous garnets are the most homogeneous garnets with almost no inclusions and are almandine-rich (40% $Fe_2O_3$, 7% MnO, 2.5% CaO and 1.5% MgO). The metamorphic garnets are more heterogeneous in composition with multiple inclusions of quartz and ilmenite and less common inclusions of plagioclase, pyrrhotite and chromite. Individual metamorphic garnets are composed of intergrown compositional domains of two general compositions: the first is a Mg-rich almandine type (33% $Fe_2O_3$, 1% MnO, 3.5% CaO and 4.5% MgO) and the second is a Ca-rich almandine garnet (37.5% $Fe_2O_3$, 1% MnO, 4% CaO and 2% MgO). These two compositions likely grew during the two amphibolite-grade metamorphic episodes that affected the Tulawaka region but it cannot be determined which garnet grew first and it was not possible to separate these two compositions during sorting.

The metamorphic garnet fractions are characterized by relatively low $^{147}Sm/^{144}Nd$ ratios (0.14-0.16) compared to the igneous garnet from the leucogranite (0.46). The low $^{147}Sm/^{144}Nd$ ratios of the metamorphic garnets are probably a product of the numerous biotite inclusions found in these garnets. The isotopic data from the metamorphic garnet fractions cannot be used for dating purposes because there is not enough spread in the $^{147}Sm/^{144}Nd$ ratio to allow an accurate regression. The initial εNd values of the metamorphic garnets range from +2.8 to -3.3 which is greater than the range found among the whole-rock samples. Regression of the leucogranite with the garnet fraction yields and age of 2.5 Ga (Fig.11) and the initial εNd value of the garnet (+5.5) is close to that of the whole-rock (+4).

**Discussion**

The compositions of the Tulawaka metavolcanic units range from tholeiitic basalt to andesite and rhyodacite and the basaltic compositions overlap those studied by Manya and Makobo (2003) in

the Bulyanhulu region of the Sukumaland greenstone belt. High Field Strength (HFS) elements such as Hf, Zr, Th, Ti and Y are often used to discriminate between tectonic environments for basalts because they are normally immobile during secondary processes and have concentrations dependent on the tectonic environment (Pearce and Cann, 1973; Wood, 1980). The Tulawaka rocks plot in the MORB/VAB field of the Pearce and Cann (1973) discrimination diagram and in the destructive plate margin in the Wood (1980) discrimination diagram (Fig. 9). These diagrams coupled with the flat to slightly light enriched REE profiles and slight LILE enrichment with positive Th and negative Ti and Nb anomalies (figures 7 and 8) support a subducted slab component in the generation of the Tulawaka basaltic rocks (Sun and McDonough, 1989; Pearce et al. 1995) and along with the basalt-andesite-dacite association are suggestive of a volcanic arc/back arc tectonic regime. The REE and trace element profiles compare well with an average profile for the Tonga Arc (Ewart et al., 1998). Manya (2001) suggested a similar origin for the Bulyanhulu basalts.

The initial Nd isotope compositions (εNd= +0.2 to +5.3) indicate that the Tulawaka metavolcanic rocks were derived from a depleted mantle, and extend the range of isotopic compositions obtained by Manya and Maboko (2003) for the Bulyanhulu basalts. The εNd value of sample DO139-2 (+5.3) is somewhat high for an Archean depleted mantle and is associated with the largest LOI value of either this study or that of Manya and Maboko (2003) and may reflect perturbation of the Sm-Nd system. The Tulawaka samples also align well with the Sm-Nd isochron generated by Manya and Maboko (2003) suggesting a similar age. The lower εNd values of the Tulawaka samples likely reflect contamination during emplacement by assimilation of sediments or alternatively, at the source by subduction of ocean floor sediments and fertilization of the mantle source by slab fluids containing a sedimentary component (DePaolo,

1981b; Scaillet and Prouteau, 2001). The question of contamination of the basaltic compositions is addressed again in the crustal evolution section below. The above data suggest an immature volcanic arc setting as a tectonic model for the origin of the Tulawaka region. This tectonic model for the Tulawaka region is in agreement with the tectonic model for the Sukumaland greenstone belt elaborated by Manya (2001).

The lower trace element and REE concentrations of the Tulawaka samples (Fig. 5 and 6) compared to the NASC is likely a product of the larger grain size of the Tulawaka metasedimentary rocks compared to the NASC (siltstone versus shale) and thus, lower clay content (Taylor and McLennan 1985). The low Zr contents of the Tulawaka sedimentary units is also evident in the Th/Sc versus Zr/Sc diagram of figure 10 which can be to study the effect of compositional variations of sedimentary sources in an active margin setting (McLennan et al., 1993). McLennan et al. (1993) observed that a rapid increase in the Zr/Sc ratio was consistent with zircon enrichment while a rapid increase in Th/Sc ratio relative to the Zr/Sc ratio reflected the contribution of a differentiated igneous source. The low Zr/Sc ratio of the Tulawaka metasedimentary samples suggests a lack of zircon enrichment, while the higher Th/Sc ratios suggest the addition of more differentiated source material. The concentration of Th, La and Sc in sedimentary rocks (Fig. 11a) can be used to discriminate between tectonic environments because their low mobility during sedimentary processes and their low residence time in sea water (Holland, 1978), resulting in little perturbation from source abundance. In figure 11a, the Tulawaka metasedimentary samples fall within the island arc field consistent with the volcanic arc origin for the Sukumaland greenstone belt postulated above and by Manya (2001). Figures 11b and 11c indicate that the metasediments of Tulawaka, despite their Archean age, are similar in composition to post-Archean pelites from the Kaapvaal craton (Jahn and Condie, 1995). The Tulawaka metasedimentary units are characterized by low Cr/Th ratios and generally low

abundances of Sc, Co and Ni (Jahn and Condie, 1995) reflecting weaker ultramafic contributions and a stronger input of granitic and mafic material compared to Archean pelites of the Kaapvaal Craton. This can be attributed to the lack of ultramafic units in the Sukumuland greenstone belt (Borg, 1992; Manya and Maboko, 2003). The low Hf (Zr) abundances corroborate the depletion in zircon noted above. The evolved nature of the sediments and lack of zircon suggests a deep off-shore depositional environment beyond the continental slope where zircon would be trapped, but still within reach of the continental sediments (Taylor and McLennan, 1985). Considering the less evolved nature of the basalts, an arc/back arc environment reminiscent of Japan/sea of Japan would seem appropriate.

The isotopic compositions of the metasedimentary rocks as well as one felsic volcanic rock yield model ages up to 3.1 Ga and lower εNd values than the mafic metavolcanic rocks. This indicates that some of the felsic volcanic units were contaminated by the sediments and that the sediments contain a detrital component significantly older than 2.8 Ga. The metasedimentary rocks are likely to be the result of a mixture between at least two sources; a basaltic source and an older differentiated source such as older granitoid rocks (Dodoman Group?).

Although the Tulawaka leucogranites are peraluminous and plot on the boundary between the "syn-collision" and "within plate granites" fields in the granite discrimination diagram (Fig. 18; Pearce et al., 1984), they are not S-type leucogranites as defined by Chapel and White (1982). In figure 19, the leucogranites plot among granites and leucogranites typical of the Western Superior Craton in Canada and the aplite in the aplite field (Breaks and Moore, 1992). The similarity in major and trace element composition between the leucogranite and aplite implies a cogenetic origin. Both have flat light REE profiles with negative Eu anomalies consistent with feldspar fractionation. The depletion in heavy REE in the aplite compared to the leucogranite

may reflect separation of the aplitic liquid from the leucogranite leaving residual minerals enriched in heavy REE. Simple fractionation calculations indicate that fractionation of small amounts of garnet with apatite from the leucogranite can reproduce the REE profile of the aplite.

The ca 2544 Ma garnet Sm-Nd age obtained for the leucogranites is substantially younger than the age of volcanism (ca. 2800 Ma; Borg and Krogh, 1999; Manya and Maboko, 2003), but is consistent with ca. 2600 Ma Rb-Sr ages for late granites of the Tanzanian Shield (Maboko and Nakamura, 1996; Rammlmair, 1990). A similar dichotomy in ages between metavolcanic rocks and associated leucogranites is observed in the Superior Province of the Canadian Shield (Ducharme et al., 1997; Larbi et al, 1999). Superior Province leucogranites are 2640 to 2680 Ma in age compared to ca 2700 to 2800 Ma for mafic volcanism and generally reflect intracrustal melting along subprovince boundaries during the final stages of the craton's amalgamation (Larbi et al., 1999; Breaks and Moore, 1992). However, the positive εNd values of the Tulawaka leucogranites indicate a strong juvenile mantle component in their formation that is inconsistent with melting of the 2800 Ma volcano-sedimentary package. Thus, the leucogranites may have formed by fractionation from a more mafic parent such as granodiorite or diorite. In addition to the Tulawaka leucogranites, Maboko and Nakamura (1996) and Rammlmair (1990) described ca. 2.6 Ga granites with juvenile Sr isotopes ratio from the Tanzanian Shield. The high $^{147}Sm/^{144}Nd$ ratios of the leucogranites and aplite are a product of extreme fractionation and it is possible that the Sm-Nd system of the aplite has been perturbed by late hydrothermal fluids. Gold mineralization at Tulawaka is found in detachment zones at the contact between the aplitic dykes and volcano-sedimentary sequences and thus post-dates the aplite and leucogranite emplacement. The 2544 Ma emplacement age for the leucogranite places an upper limit on the age of gold mineralization. This upper limit is 100 million years younger than the upper limit for gold

mineralization at the Geita mine (2644 Ma; Borg and Krogh, 1999), but both ages indicate that gold mineralization in the Sukumuland greenstone belt post-date the main volcanic events.

*Crustal evolution and regional comparisons*

The evolution of the Tulawaka region is comparable, but slightly different from the evolution of other greenstone belt sequences of the African continent. For example, the lack of ultramafic komatiitic rocks at Tulawaka compared to those found in greenstone belts of the Kaapvaal craton (Wilson and Carlson, 1989) or within the Reguibat Rise of the West African craton (Potrel et al., 1998). The major crustal growth period of the Sukumaland greenstone belts occurred between 2.7 and 3.0 Ga (Borg and Krogh, 1999; Manya and Makobo, 2003; this study) and is younger than the growth period for the Kaapvaal craton greenstone belt sequences (2.9-3.0 Ga; Wilson and Carlson, 1989) but is similar in age with the growth period of the West African craton sequences (2.7-3.0 Ga; Potrel et al., 1998) and the Harare-Shamva greenstone belts (2.7-2.6 Ga; Jelsma et al. 1996)of the Zimbabwe craton. Model ages of metasedimentary rocks at Tulawaka indicate an older basement source of ~3.0 Ga comparable to the 3.2-2.8 Ga age found by Dougherty-Page (1994) for the Harare-Shamva greenstone belt. The Kaapvaal and West African cratons have an older basement age of ~3.6 and 3.5 Ga, respectively (Compston and Kröner, 1988; Jelsma et al., 1989). The Sukumaland greenstone belt, therefore seems to be more similar to the Harare-Shamva greenstone belts found in the north of the Zimbabwe craton with similar basement and crustal evolution ages. Figure 20 (εNd versus time) illustrates how the isotopic compositions of the Tanzanian Craton overlap those of the Zimbabwe Craton while the Kaapvaal and West African cratons lie at lower (older) isotopic compositions.

## Conclusions

The geochemistry and Sm-Nd isotope compositions were obtained from metasedimentary and metavolcanic units, leucogranites and an aplite from the Tulawaka East deposit in the Sukumuland greenstone belt of the Tanzanian Shield. The basalt-andesite-dacite association, positive initial εNd values, negative Nb anomalies and otherwise flat REE and trace element patterns indicate that the metavolcanic rocks were extracted from an Archean depleted mantle in an immature volcanic arc/back-arc setting. The Nd isotope compositions of the metavolcanic rocks are consistent with the ca. 2.8 Ga ages obtained for early volcanism in the Sukumaland greenstone belt (Borg and Krogh, 1999; Manya and Maboko, 2003). Trace element abundances and Nd isotope compositions suggest that the metasedimentary rocks represent a mixture between a juvenile detrital component (the metavolcanic rocks) and an older differentiated detrital component (the Dodoman Group?). The leucogranites have juvenile isotopic compositions and are likely the differentiation product of a more mafic magma. The aplite is cogenetic with the leucogranites and is probably the result of a late stage differentiate of the leucogranitic magma produced by fractionation of garnet and apatite.

A garnet/whole rock isochron of 2544 Ma for the leucogranite is broadly consistent with the age of late granite plutonism in the region (Rammlmair et al., 1990; Mokobo and Nakamura, 1996) and places an upper limit on the age of gold mineralization in the Tulawaka East deposit. This age likely also coincides with the local amphibolite grade of metamorphism related to the emplacement of granitic plutons. The Nd isotopic data indicates that the isotopic evolution of the Tanzanian shield closely resembles that of the Zimbabwe craton and is younger than the Kaapvaal craton.

## Acknowledgments

The authors wish to thank Gerald Panneton of Pangea Goldfields ltd and Carlos Bertoni of Northern Mining and Exploration for providing the opportunity to study the Tulawaka rocks. This study was supported by a grant from the Natural Sciences and Engineering Research Council of Canada to RKS and by a graduate research scholarship from the Université du Québec à Montréal to JC.

**References**

Abouchami, W., Boher, M., Michard, A., Albarède, F., 1990. A major 2.1 Ga event mafic magmatism in West Africa: An early stage of crustal accretion. Journal of Geophysical Research, 95 (B11) : 17605-17629.

Albarède, F., 1998. The growth of the continental crust. Tectonophysics, 296 : p. 1-14.

Anders, E., Grevesse N., 1989. Abundances of the elements: Meteoritic and solar. Geochimica et Cosmochimica Acta, 53-1, 197-214.

Bardoux, M., 2001. Geology of the Tulawaka deposit, North-Central Tanzania. An update. 14 p. Technical report submitted to Pangea Goldfields ltd. and Northern Mining Exploration ltd.

Barth, H., 1987. Assessment of the regional geology, gold and base metal potential in the Lake Victoria region, Tanzania. BRG, Hanover (unpublished).

Bell, K., Dodson, M. H., 1981. The Geochronology of the Tanzanian Shield. The Journal of Geology 89 : 109-128.

Bhatia, M. R., Crook, K. A. W., 1996. Trace element characteristics of greywackes and tectonic setting discrimination of sedimentary basins. Contributions to Mineralogy and Petrology, 92:

181-193.

Borg, G., 1992. New aspects of lithostratigraphy and evolution of the Siga Hills, an Archean granite-greenstone terrain in NW Tanzania. Zeitschrift Angewandte Geologie, 38 : 89-93.

Borg, G., 1993. The Geita gold deposits, NW-Tanzania. Geology, ore petrology, geochemistry and timing of events. Geologisches Jahrbuch, D100 : 545-595.

Borg, G., Krogh, T., 1999. Isotopic age data of single zircons from Archean Sukumaland Greenstone belt, Tanzania. Journal of African Earth Sciences, 29 (2) : 301-312.

Borg, G., Lyatuu, D. R., Rammlmair, D., 1990. Genetic aspects of the Geita and Jubilee reef, Archean BIF-hosted gold deposits, Tanzania. Geologische Rundschau, 79 : 355-371.

Borg, G. and Shackelton, R. M., 1997. The Tanzania and NE Zaire cratons. Oxford : 608-619.

Breaks, F. W., Moore, J. M., 1992. The Ghost Lake batholith, Superior Province of northwestern Ontario: A fertile S-type, peraluminous granite-rare element pegmatite system. Canadian Mineralogist, 30 : 835-875.

Chappel, B. W., White, A. J. R., 1982. I- and S-type granites in the Lachlan fold belt, southern Australia. Science Press, Beijing, China : 87-101.

Clifford, T. N., 1970, The structural framework of Africa. Edinburgh: 1-26.

Compston, W., Kröner, A., 1988. Multiple zircon growth within early Archean tonalite gneiss from the Ancient Gneiss Complex, Swaziland. Earth and Planetary Science Letters, 87: 13-28.

Condie, K.C., 1989. Plate Tectonics and Crustal Evolution. Pergamon, Oxford, 476 pp.

DePaolo, D.J., 1981a. Neodymium isotopes in the Colorado Front Range, and crust-mantle evolution in the Proterozoic. Nature, 291 : 193-196.

DePaolo, D.J., 1981b. Trace element and isotopic effects of combined wallrock assimilation and fractional crystallization. Earth and Planetary Science Letters, 53 : 189-202.

Dougherty-Page, J. S., 1994. The evolution of the Archean continental crust of northern Zimbabwe (unpublished). PhD thesis, Milton Keynes, Open University, 244p.

Ducharme, Y., Stevenson, R.K., Machado, N., 1997. Sm-Nd geochemistry and U-Pb geochronology of the Preissac and Lamotte leucogranites, Abitibi Subprovince. Canadian Journal of Earth Sciences, 34 : 1059-1071.

Ewart, A., Collerson, K. D., Regelous, K., Wendt, J. I., Niu Y., 1998. Geochemical Evolution within the Tonga-Kermadec-Lau Arc-Back-arc Systems: the Role of Varying Mantle Wedge Composition in Space and Time. Journal of Petrology, 39 : 331-368.

Gabert, G., 1990. Lithosratigraphic and Tectonic Setting of Gold Mineralization in the Archean Cratons of Tanzania and Uganda, East Africa. Precambrian Research, 46 : 59-69.

Goldfarb, R. J., Groove, D. I., Gardoll, S., 2001. Orogenic gold and geologic time: a global synthesis. Ore Geology Reviews, 18 : 1-75.

Gromet, L. P., Dymek, R. F., Haskin, L. A., Korotev, R. L., 1984. The "North American shale composite": Its compilation, major and trace element characteristics. Geochimica et Cosmochimica Acta, 48 : 2469-2482.

Gruau, G., Chauvel, C., Jahn, B.M., 1990. Anomalous Sm-Nd ages for the early Archean

Onverwacht Group volcanics. Contributions to Mineralogy and Petrology, 104 : 27-34.

Harpum, J. R., 1956. Summary of the geology of Tanganyika; part V: Structure and geotectonics of Precambrian. Geological Survey of Tanganyika, mem. 2, Dar-es-Salaam.

Henry, P., Stevenson, R. K., Gariépy, C., 1998. Late Archean mantle composition and crustal growth in the Western Superior Province of Canada : Neodymium and lead isotopic evidence from the Wawa, Quetico and Wabigoon subprovinces. Geochimica et Cosmochimica Acta 62, 143-157.

Holland, H.D., 1978. The chemistry of the atmosphere and oceans. Wiley, New York.

Jahn, B.-M., Condie, K. C., 1995. Evolution of the Kaapvaal Craton as viewed from geochemical and Sm-Nd isotopic analyses of intracratonic pelites. Geochimica et Cosmochimica Act 59, 2239-2258.

Jelsma, H. A., Vinyu, M. L., Valbracht, P. J., Davies, G. R., Wijbrans, J. R., and Verdumen, E. A. T., 1996. Constraints on Archean crustal evolution of the Zimbabwe craton: a U-Pb zircon, Sm-Nd and Pb-Pb whole-rock isotope study. Contributions to Mineralogy and Petrology 124, 55-70.

Kuehn, S., Ogola, J., Sango, P., 1990. Regional setting and nature of gold mineralization in Tanzania and southwest Kenya. Precambrian Research 46, 71-82.

Larbi, Y.; Stevenson, R.K.; Breaks, F.; Machado, N.; Gariépy, C., 1999. Age and isotopic composition of late Archean leucogranites : implications for continental collision in the western Superior Province. Canadian Journal of Earth Sciences 36, 495-510.

Lenoir, J. L., Liégeois, J-P. Theunissen, K., Klerkx, J., 1994. The Paleoproterozoic Ubendian shear belt in Tanzania: geochronology and structure. Journal of African Earth Sciences 19, 169-184.

Makobo, M. A. H., Nakamura, E., 1996. Nd and Sr isotopic mapping of the Archean-Protezocoic boundary in southeastern Tanzania using granites as probes for crustal growth. Precambrian Research 77, 105-115.

Manya, S., 2001. Geochemical investigation of Archean greenstones in Rwamagaza area, north-western Tanzania. Msc. Thesis, University of Dar es Salaam.

Manya, S., Maboko, M. A. H., 2003, Dating basaltic volcanism in the Neoarchean Sukumaland Greenstone Belt of the Tanzania Craton using the Sm-Nd method : implications for the geological evolution of the Tanzania Craton. Precambrian Research 121, 35-45.

McLennan, S. M., Hemming, S., McDaniel, D. K., Hanson, G. N., 1993, Geochemical approaches to sedimentation, provenance and tetonics: Boulder, Colorado, Geological Society of America, Special Paper 284, 21-40.

Meschede, M., 1986. A method of discriminating between different types of mid-ocean ridge basalts and continental tholeiites with Nb-Zr-Y diagram. Chemical Geology 56, 207-218.

Patchett, P. J., Arndt, N. T., 1986. Nd isotopes and tectonics of 1.9-1.7 Ga crustal genesis. Earth and Planetary Science Letters 78, 329-338.

Pearce, J. A., Cann, J. R., 1973. Tectonic setting of basic volcanic rocks determined using trace element analyses 19, 290-300.

Pearce, J. A., Harris, N. B. W., Tindle, A. G., 1984. Trace element discrimination diagrams for the tectonic interpretation of granitic rocks. Journal of Petrology 25, 956-983.

Pearce, J.A.; Peate, D.W., 1995. Tectonic implication of the composition of volcanic arc magmas. Annual Reviews of Earth and Planetary Sciences 23, 251-285.

Potrel, A., Peucat, J. J., Fanning, C. M., 1998. Archean crustal evolution of the West African Craton: Example of the Amsaga Area (Reguibat Rise). U-Pb and Sm-Nd evidence for crustal growth and recycling. Precambrian Research 107, 107-117.

Rammlmair, D.; Höhndorf, A.; Borg, G.; Hiza, G.N, 1990. Nouvelles datations isotopiques des granites et des gabros de la région "greenstone"-granitique du Sukumaland, N.W.-Tanzania (abstract volume). 15th Colloquium of African Geology, Nancy 43.

Richard, P., Shimizu, N., Allčgre, J. J., 1976. A natural tracer: an application to oceanic basalts. Earth and Planetary Science Letters 31, 269-278.

Ring, U., 1993. Aspects of the kinematic history and mechanisms of superposition of the Proterozoic mobile belts of eastern Central Africa (northern Malawi and southern Tanzania). Precambrian Research 62, 207-226.

Robinson, S. D., Aubertin, R. A., 2000. Prelimininary report on re-logging of diamond drill core (East zone gold deposit). Pangea Minerals (Tanzania) limited - Tulawaka Project. 24 p.

Scaillet, B., Prouteau, G., 2001. Oceanic slab melting and mantle metasomatism. Science Progress 84, 335-354.

Shand, S. J., 1927, Eruptive rocks : their genesis composition, classification, and their relation to

ore-deposits. With a chapter on meteorites.: (1949) 3rd edition, London, 488p.

Stevenson, R.K., Patchett, P.J., 1990. Hf isotopic evidence for the evolution of the early crust. Geochimica et Cosmochimica Acta 59,

Stockley, G. M., 1935 Outline of the geology of the Musoma district. Geological Survey of Tanganyika 7, 1-64.

Stockley, G. M., 1948. The geology and mineral resources of Tanganyika Territory. Geological Survey of Tanganyika 20, 1-37.

Sun, S. S., McDonough, W. F., 1989. Chemical and isotopic systematic of oceanic basalts. Implication for mantle composition and processes. p. 313-345.

Tassel, A., 2003. Tanzania's gold boom continues. African Mining 8.

Taylor, P.N., Kramers, J.D., Moorbath, S., Wilson, J.F., Orpen, J.L., Martin, A., 1991. Pb/Pb, Sm-Nd and Rb-Sr geochronology in the Archean craton of Zimbabwe. Chemical Geology (Isotope Geoscience Section) 87, 175-196.

Taylor, S.R., McLennan, S.M., 1985. The Continental Crust: Its Composition and Evolution. Blackwell, Oxford.

Thompson, P. H., 2002. Second Report on the Petrography of Tulawaka Samples: Implications for metamorphic conditions, stratigraphy, deformation and mineralization. Peter H. Thompson Geological Consulting Ltd, submitted to Pangea Goldfields ltd. and Northern Mining Exploration ltd., 26 p.

Wade, F. B. and Oates, F., 1938. An explanation of the degree sheet No. 52, Dodoma. Geological

Survey of Tanganyika 17, 1-60.

Wilson, A. H., Carlson, R. W., 1989. A Sm-Nd and Pb isotope study of Archean greenstone belts in the southern Kaapvaal Craton, South Africa. Earth and Planetary Science Letters 96, 89-105.

Winchester, J. H., Floyd, P. A., 1977. Geochemical discrimination of different magma series and their differentiation products using immobile elements. Chemical Geology 20, 325-343.

Wood, D. A., 1980. The application of a Th-Hf-Ta diagram to problems of tectonomagmatic classification and to establishing the nature of crustal contamination of basaltic lavas of the British Tertiary volcanic Province. Earth and Planetary Science Letters 50, 11-30.

Wronkiewicz, D. J., Condie, K. C., 1990. Geochemistry and mineralogy of sediments from the Vendersdorp and Transvaal Supergroup, South Africa : Cratonic evolution during the early Proterozoic. Geochimica et Cosmochimica Acta 54, 343-354.

Yager, T. R., 2000. The mineral industry of Tanzania. US geological survey minerals, yearbook 2000, 28.1-28.4.

**Figures Captions**

Figure 1: Geological map of Tanzania (modified from the mineral resource department of Tanzania).

Figure 2: Geological map of Lake Victoria district and Sukumaland greenstone belt (modified from Northern Mining ltd).

Figure 3: Winchester and Floyd (1977) diagram for the volcanic rocks of Tulawaka East prospect.

Figure 4: Major element variation diagrams of SiO2 versus MgO (A), TiO2 (B), K2O (C), Fe2O3 (D), CaO (E) and Al2O3 (F) for metasedimentary rocks (□), metavolcanic rocks (mafic ◆ and felsic ◈), leucogranites (△) and aplite (●) of Tulawaka East with the field of basaltic rocks of Manya and Maboko (2003).

Figure 5: REE profiles for (A) sedimentary rocks with NASC profile (Gromet et al., 1984), (B) felsic volcanic rocks, (C) mafic volcanic rocks with N-MORB (Sun and McDonough, 1989) and young arc (Tonga) (Ewart et al., 1998) profiles and (D) leucogranites and the aplite dyke. Chondrite normalization values from Anders and Grevesse (1989).

Figure 6: Trace element profiles for (A) sedimentary rocks with NASC profile (Gromet et al., 1984), (B) felsic volcanic rocks, (C) mafic volcanic rocks with N-MORB (Sun and McDonough,

1989) and young arc (Tonga) (Ewart et al., 1998) profiles and (D) leucogranites and the aplite dyke.

Figure 7. (a) 143Nd/144Nd versus 147Sm/144Nd diagram for the metasedimentary rocks (□), the metavolcanic rocks (mafic ◆ and felsic ◈) and the leucogranites (△) of Tulawaka East with the isochron obtained by Manya and Maboko (2003) on metabasalts. (b) 143Nd/144Nd versus 147Sm/144Nd diagram for whole-rock and garnet fractions of Tulawaka East.

Figure 8. (a) Pearce and Cann (1973) discrimination diagram for the metavolcanic basalts of Tulawaka (VAB : Volcanic Arc Basalt, WPB : Within Plate Basalt, MORB : Mid-Ocean Ridge Basalt). (b) Wood (1980) discrimination diagram for the metavolcanic basalts of Tulawaka.

Figure 9. A Th/Sc versus Zr/Sc plot (McLennan et al., 1993) of metasedimentary rocks indicates that the Tulawaka rocks are depleted in Zr and enriched in Th compared to modern turbidite sequences. This likely reflects a deeper water environment where with a larger clay/heavy mineral (zircon) ratio.

Figure 10. (a) A Hf-Th-Co diagram (Wronkiewicz and Condie, 1990) for Tulawaka metasedimentary rocks indicates with the fields of Tulawaka basalts, leucogranites and Archean and post-Archean pelites of Kaapvaal craton (Jahn and Condie, 1995). Gr : granite, Ton: tonalite, Kom: komatiite and NASC: North American shale composite.
(b) Bhatia and Crook (1986) discrimination diagram for the metasedimentary rocks present at Tulawaka East. A : Oceanic island arc; B : Continental island arc; C : Active continental margin and D : Passive margin. (c) Chemical composition of Tulawaka metasedimentary rocks on Th-

La-Sc diagram (after Wronkiewickz and Condie, 1990) with the fields of Tulawaka basalts, leucogranite and Archean and post-Archean pelites of Kaapvaal craton (Jahn and Condie, 1995). Gr : granite, Ton: tonalite, Kom : komatiite and NASC : North American shale composite.

Figure 11: εNd versus Nd diagram for metasedimentary rocks (□), the metavolcanic rocks (mafic ◆ and felsic ◈) and the leucogranites (△) present at Tulawaka Eat with the field of basaltic rocks from Manya and Maboko (2003).

Figure 12: (a) Pearce et al. (1984) discrimination diagram for the leucogranites present at Tulawaka East. (b) K2O versus Na2O variation diagram for the leucogranites (△) and aplite (●) with the fields of granites and aplites of Western Superior (Breaks and Moore, 1992) and S-type granites of Lachlan belt (Chappel and White, 1982).

Figure 13: εNd versus time for the metasedimentary rocks (□), the metavolcanic rocks (mafic ◆ and felsic ◈) and the leucogranites (△) with the fields of Kaapvaal Craton (Wilson and Carlson, 1989; Gruau et al., 1990; Jahn and Condie, 1995), West African Craton (Potrel et al., 1998; Aboumachi et al., 1990), Zimbabwe Craton (Taylor et al., 1991; Jelsma et al. 1996) and Tanzania Craton (Maboko and Nakamura, 1996; Manya and Makobo, 2003; this study). εNd values were calculated at 2.8 Ga for metasedimentary and metavolcanics rocks and at 2.5 Ga for the leucogranites.

## Table captions

Table 1: Major element compositions of the rock types from the Tulawaka East gold deposit (in %)

Table 2: Minor element compositions of the rock types from the Tulawaka East gold deposit (in ppm)

Table 3: Sm-Nd isotopic data of rock types from the Tulawaka East gold deposit

**Figure 1**

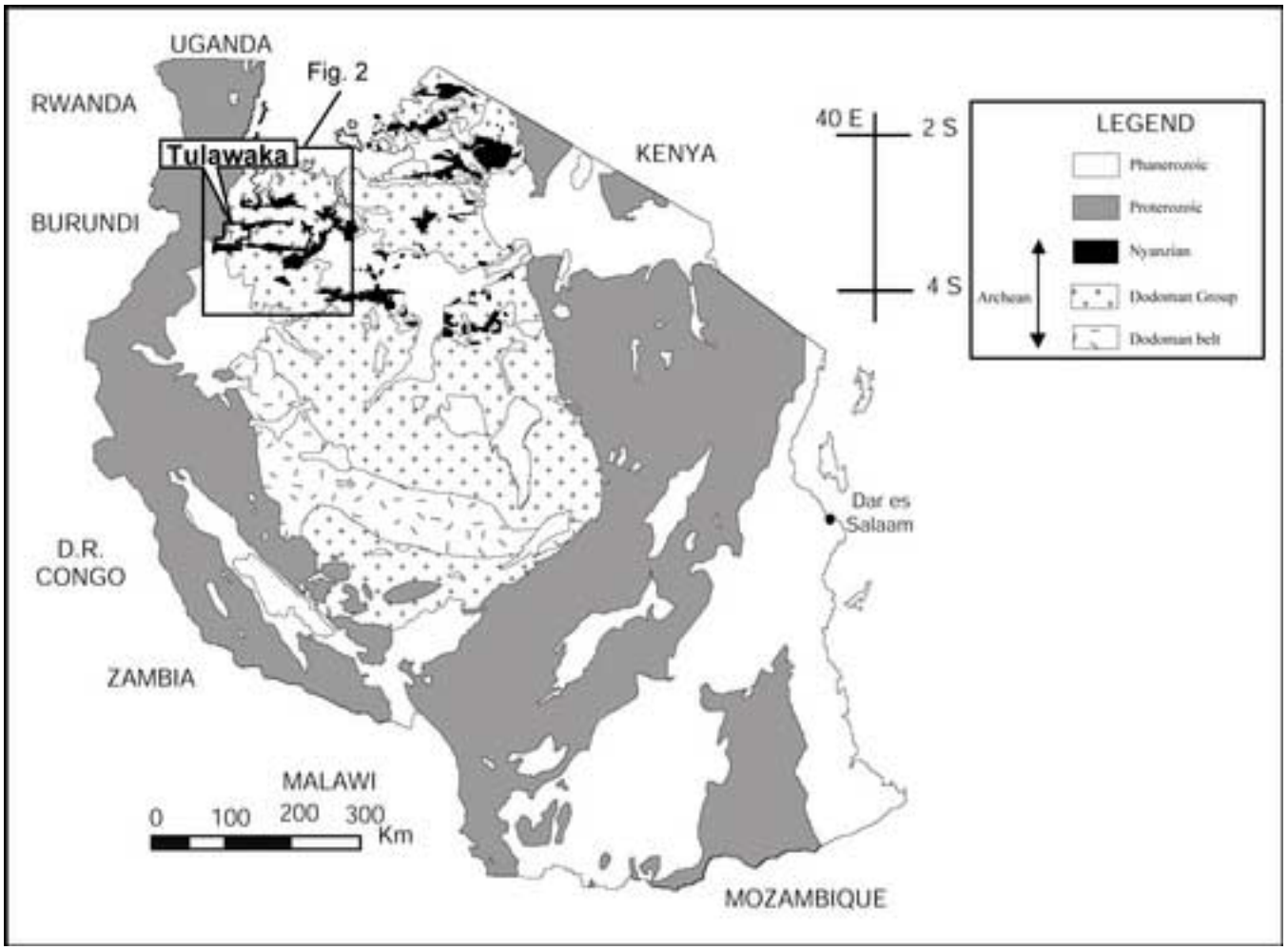
UGANDA
RWANDA
BURUNDI
Fig. 2
Tulawaka
KENYA
40 E
2 S
4 S
LEGEND
Phanerozoic
Proterozoic
Nyanzian
Archean
Dodoman Group
Dodoman belt
Dar es Salaam
D.R. CONGO
ZAMBIA
MALAWI
0 100 200 300 Km
MOZAMBIQUE

**Figure 2**

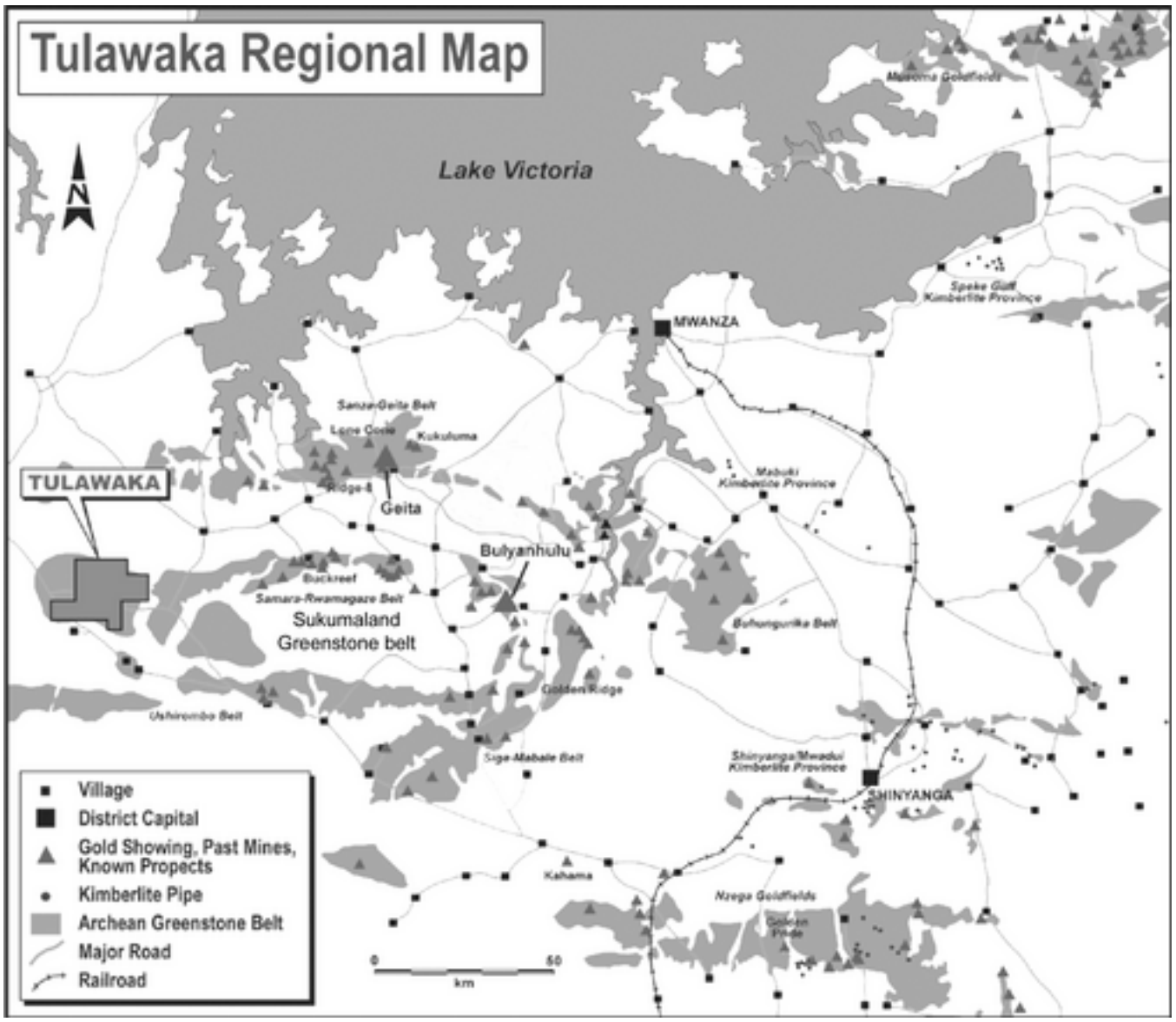
Tulawaka Regional Map
Lake Victoria
N
MWANZA
Speke Gulf Kimberlite Province
Mabuki Kimberlite Province
Sanza-Geita Belt
Lone Cone
Kukuluma
Ridge 4
Geita
TULAWAKA
Bulyanhulu
Buckreef
Samara-Rwamagaza Belt
Sukumaland Greenstone belt
Golden Ridge
Ushirombo Belt
Suge-Mabale Belt
Buhunguriko Belt
Shinyanga/Mwadui Kimberlite Province
SHINYANGA
Kahama
Nzega Goldfields
Village
District Capital
Gold Showing, Past Mines, Known Propects
Kimberlite Pipe
Archean Greenstone Belt
Major Road
Railroad
0
50
km

**Figure 3**

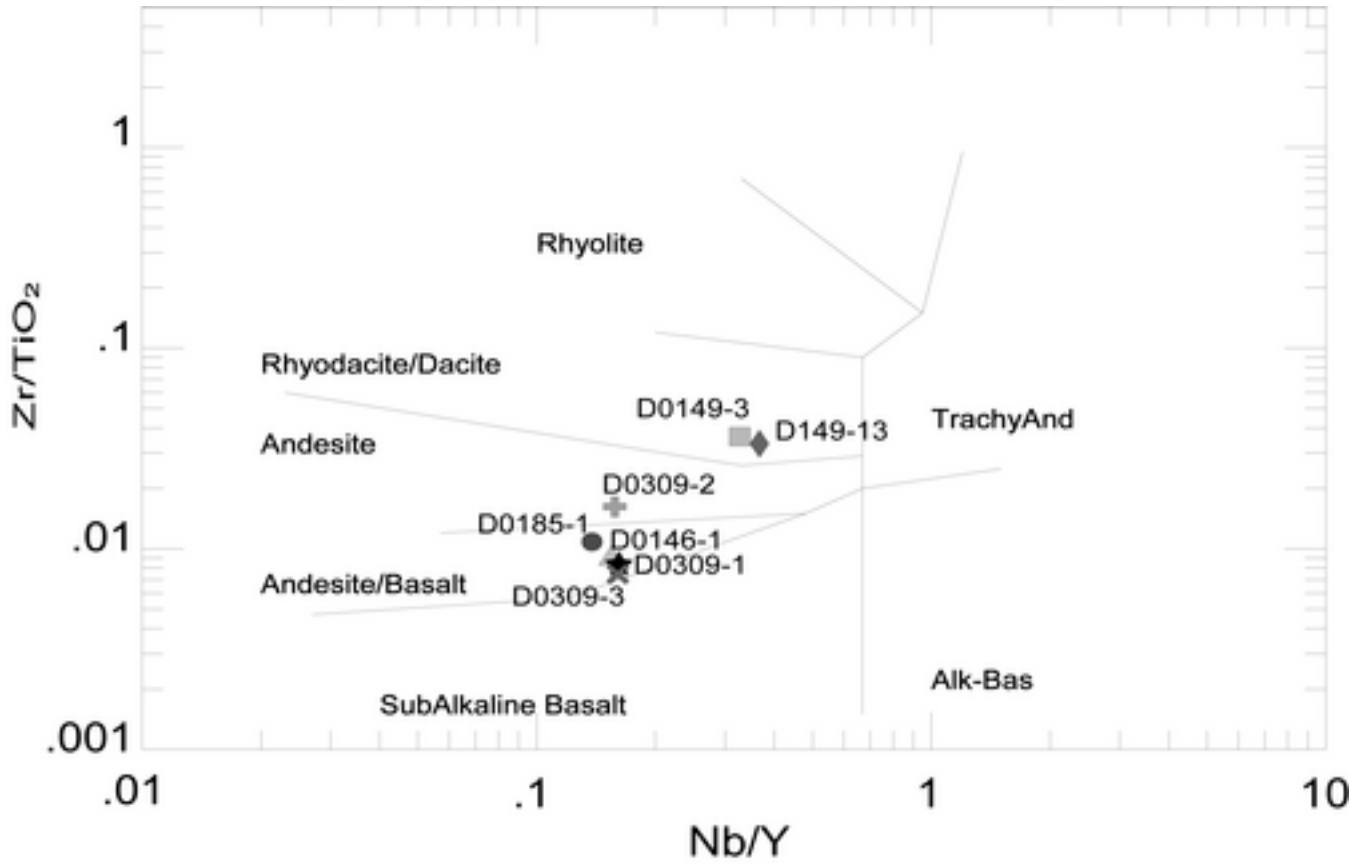
1
.1
.01
.001
Zr/TiO2
Rhyolite
Rhyodacite/Dacite
Andesite
Andesite/Basalt
SubAlkaline Basalt
TrachyAnd
Alk-Bas
D0149-3
D149-13
D0309-2
D0185-1
D0146-1
D0309-1
D0309-3
.01
.1
1
10
Nb/Y

**Figure 4**

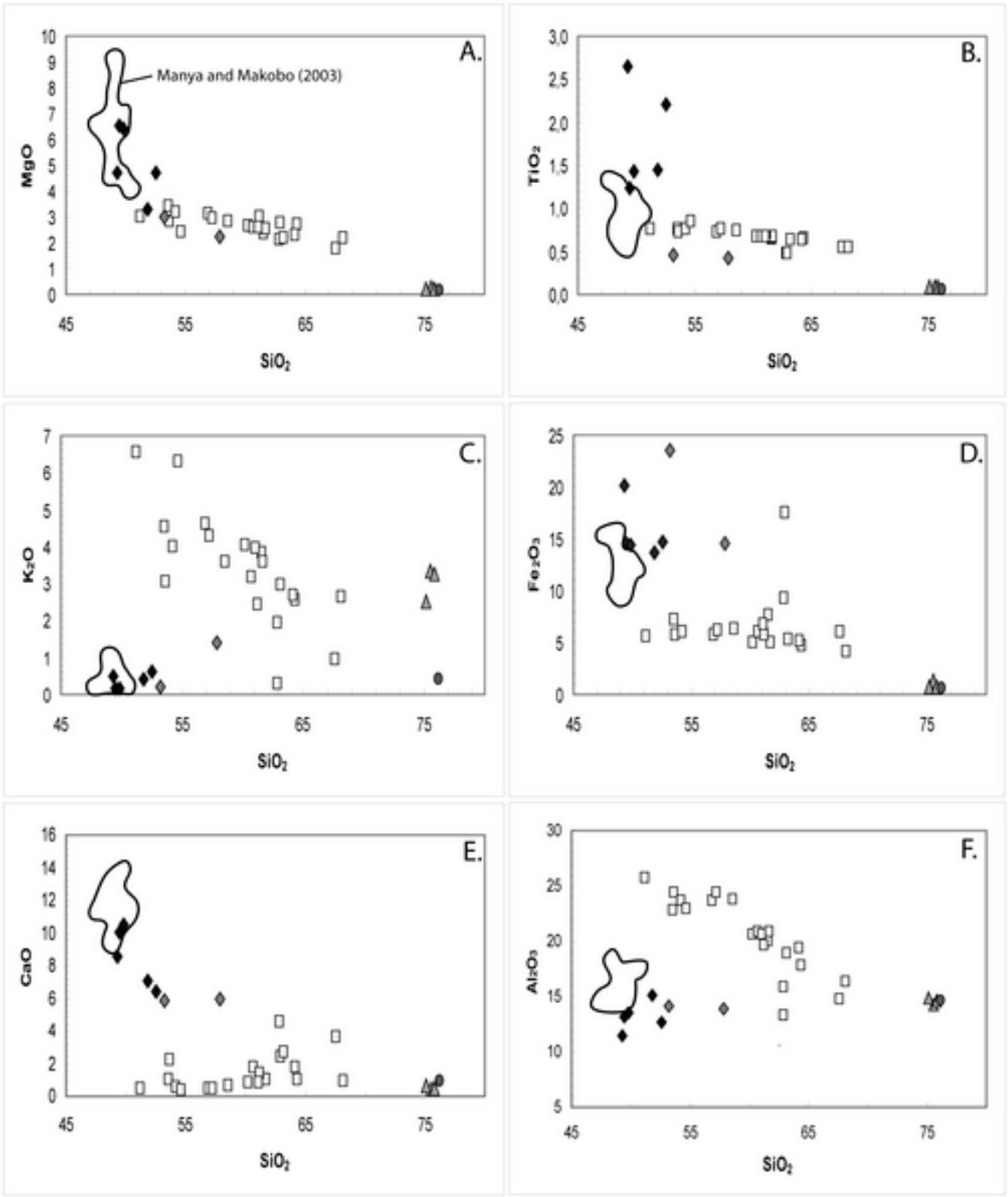
A.
Manya and Makobo (2003)
MgO
SiO2
B.
TiO2
SiO2
C.
K2O
SiO2
D.
Fe2O3
SiO2
E.
CaO
SiO2
F.
Al2O3
SiO2

**Figure 5**

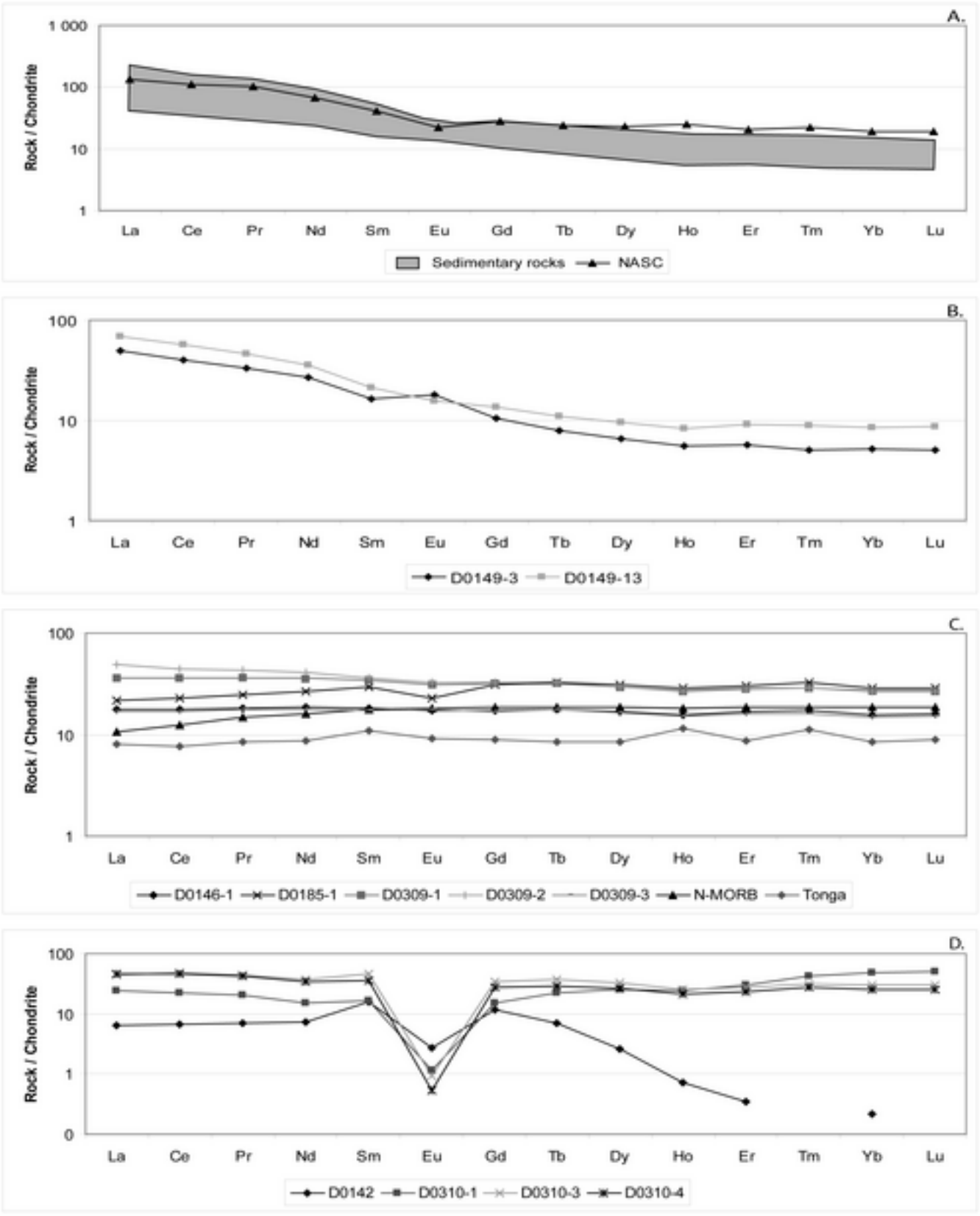
A.
1 000
100
10
1
Rock / Chondrite
La Ce Pr Nd Sm Eu Gd Tb Dy Ho Er Tm Yb Lu
Sedimentary rocks
NASC
B.
100
10
1
Rock / Chondrite
La Ce Pr Nd Sm Eu Gd Tb Dy Ho Er Tm Yb Lu
D0149-3
D0149-13
C.
100
10
1
Rock / Chondrite
La Ce Pr Nd Sm Eu Gd Tb Dy Ho Er Tm Yb Lu
D0146-1
D0185-1
D0309-1
D0309-2
D0309-3
N-MORB
Tonga
D.
100
10
1
0
Rock / Chondrite
La Ce Pr Nd Sm Eu Gd Tb Dy Ho Er Tm Yb Lu
D0142
D0310-1
D0310-3
D0310-4

**Figure 6**

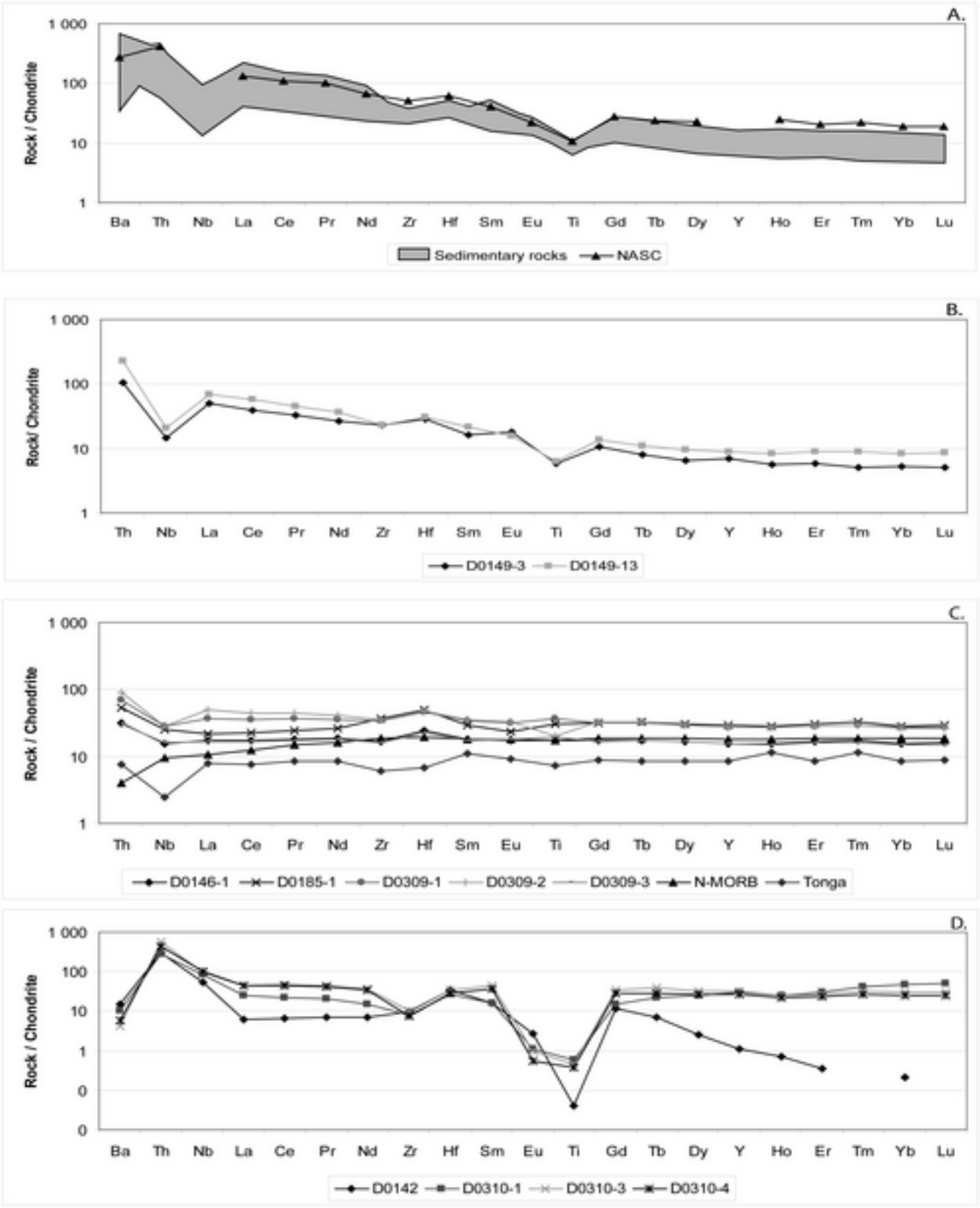
A.
1 000
100
10
1
Rock / Chondrite
Ba Th Nb La Ce Pr Nd Zr Hf Sm Eu Ti Gd Tb Dy Y Ho Er Tm Yb Lu
Sedimentary rocks
NASC
B.
1 000
100
10
1
Rock/ Chondrite
Th Nb La Ce Pr Nd Zr Hf Sm Eu Ti Gd Tb Dy Y Ho Er Tm Yb Lu
D0149-3
D0149-13
C.
1 000
100
10
1
Rock / Chondrite
Th Nb La Ce Pr Nd Zr Hf Sm Eu Ti Gd Tb Dy Y Ho Er Tm Yb Lu
D0146-1
D0185-1
D0309-1
D0309-2
D0309-3
N-MORB
Tonga
D.
1 000
100
10
1
0
0
Rock / Chondrite
Ba Th Nb La Ce Pr Nd Zr Hf Sm Eu Ti Gd Tb Dy Y Ho Er Tm Yb Lu
D0142
D0310-1
D0310-3
D0310-4

**Figure 7**

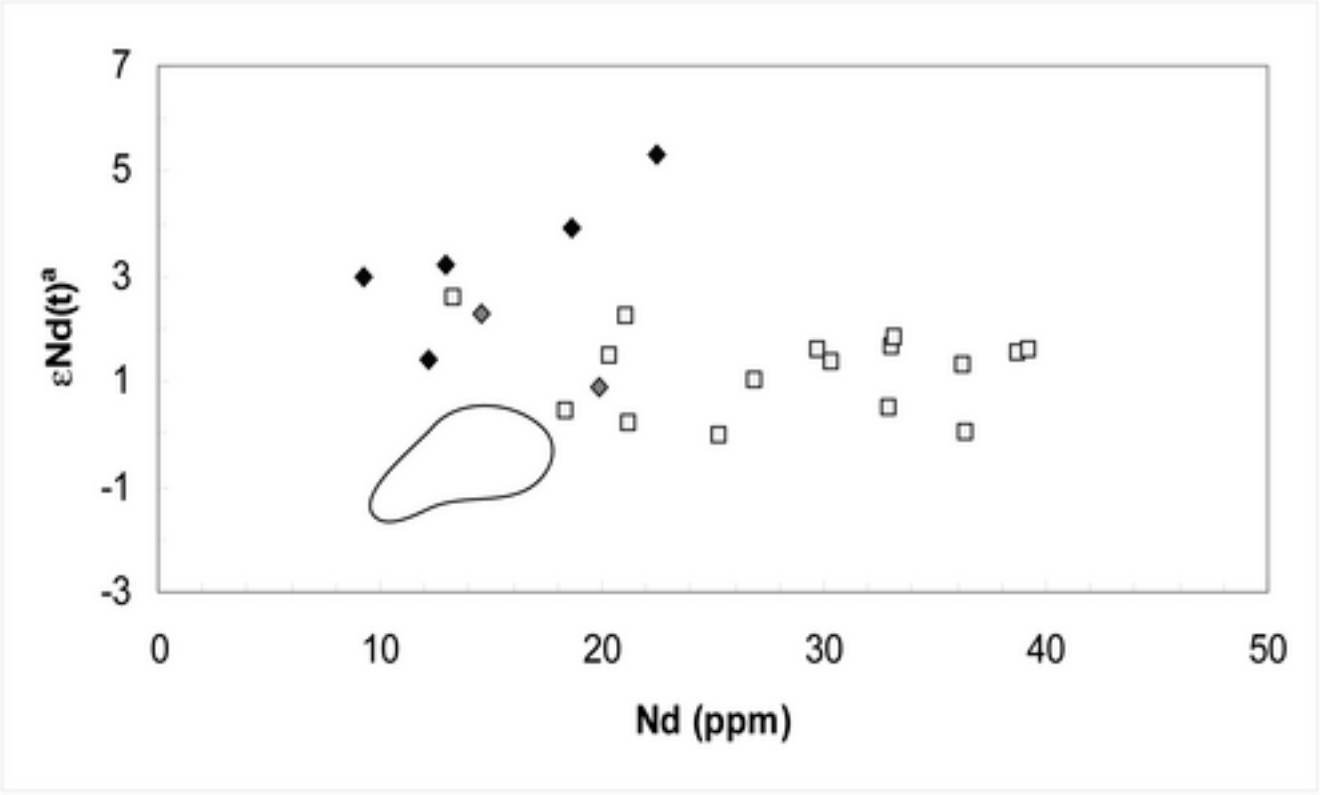

**Figure 8**

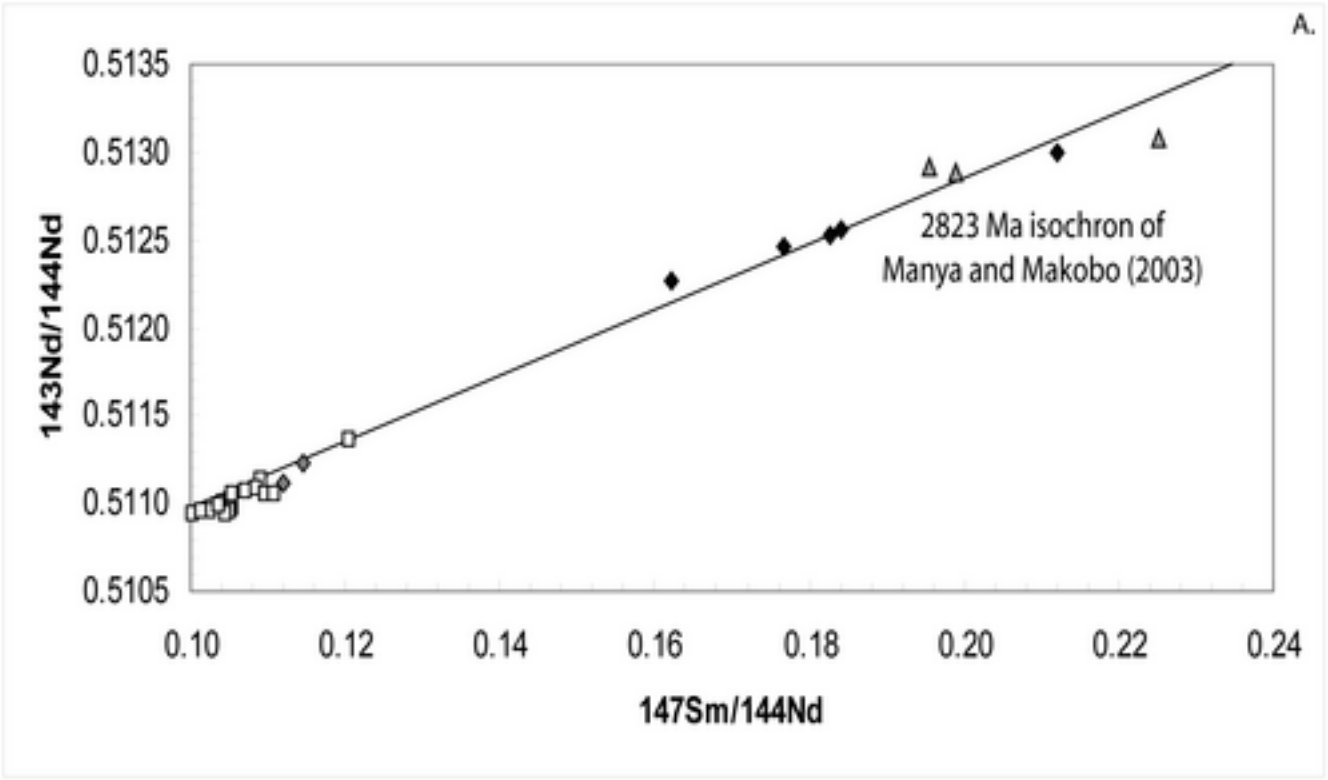
A.
0.5135
0.5130
0.5125
0.5120
0.5115
0.5110
0.5105
143Nd/144Nd
2823 Ma isochron of
Manya and Makobo (2003)
0.10
0.12
0.14
0.16
0.18
0.20
0.22
0.24
147Sm/144Nd

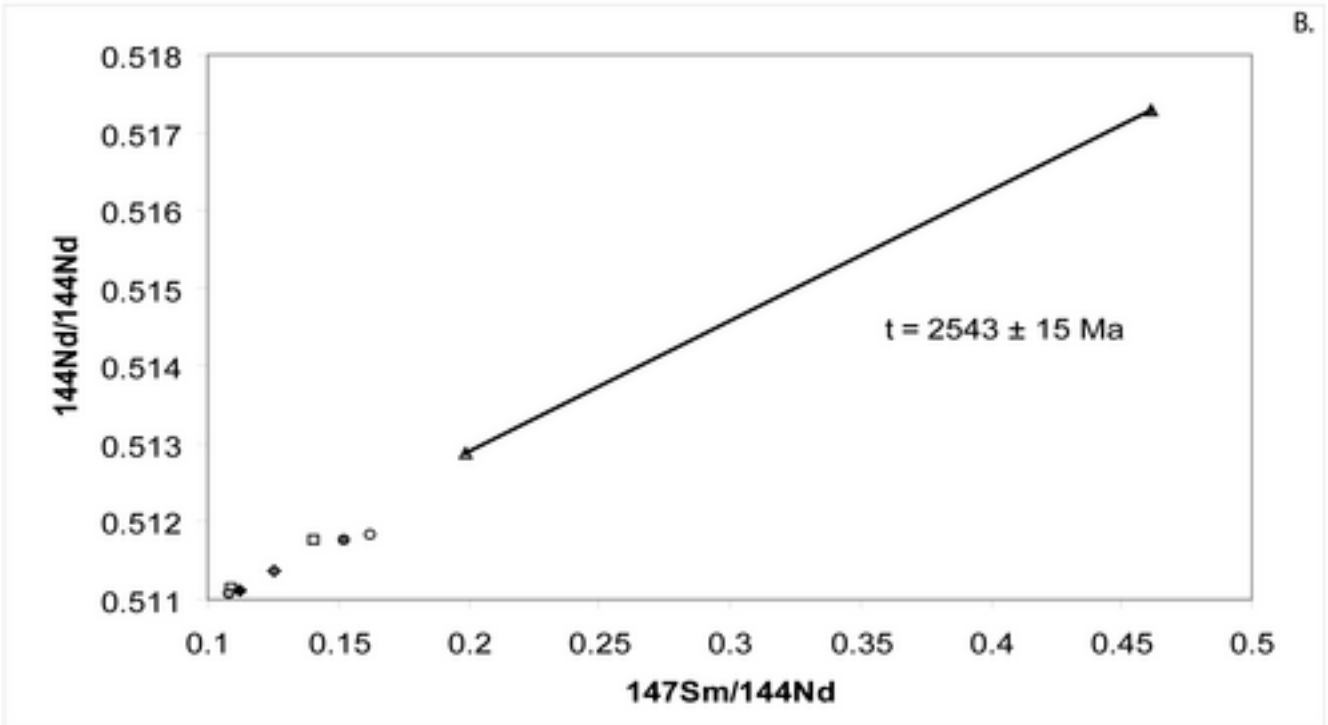
B.
0.518
0.517
0.516
0.515
0.514
0.513
0.512
0.511
144Nd/144Nd
t = 2543 ± 15 Ma
0.1
0.15
0.2
0.25
0.3
0.35
0.4
0.45
0.5
147Sm/144Nd

**Figure 9**

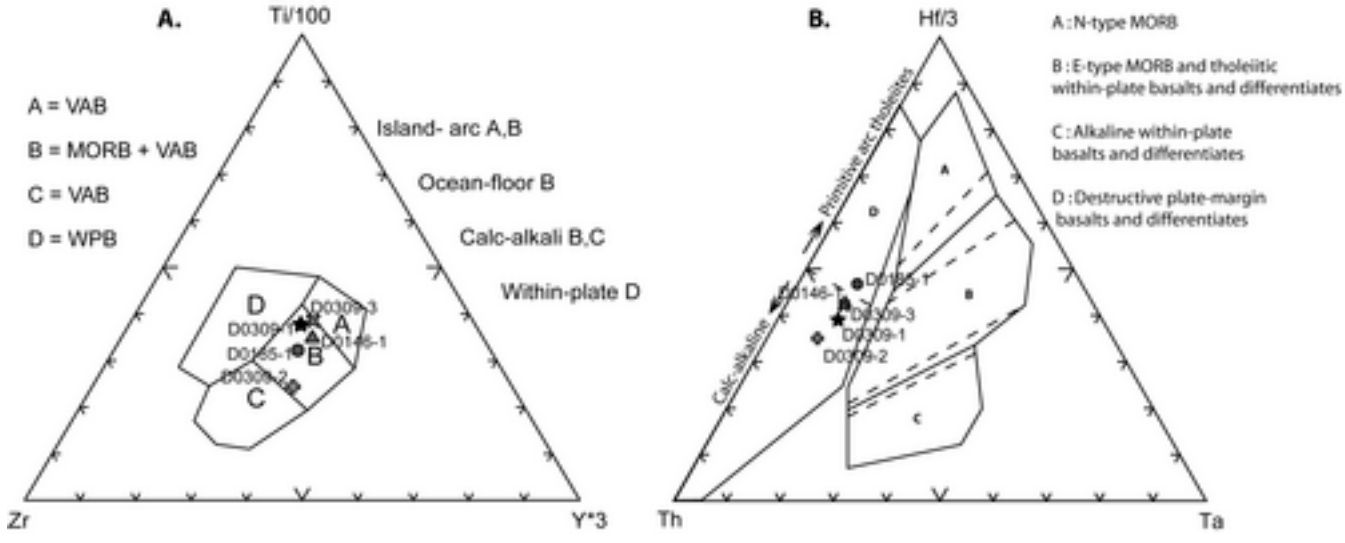
A.
Ti/100
A = VAB
B = MORB + VAB
C = VAB
D = WPB
Island- arc A,B
Ocean-floor B
Calc-alkali B,C
Within-plate D
D0309-3
D0309-1
D0146-1
D0165-1
D0309-2
Zr
Y*3
B.
Hf/3
Primitive arc tholeiites
Calc-alkaline
D0146-1
D0165-1
D0309-3
D0309-1
D0309-2
Th
Ta
A : N-type MORB
B : E-type MORB and tholeiitic within-plate basalts and differentiates
C : Alkaline within-plate basalts and differentiates
D : Destructive plate-margin basalts and differentiates

**Figure 10**

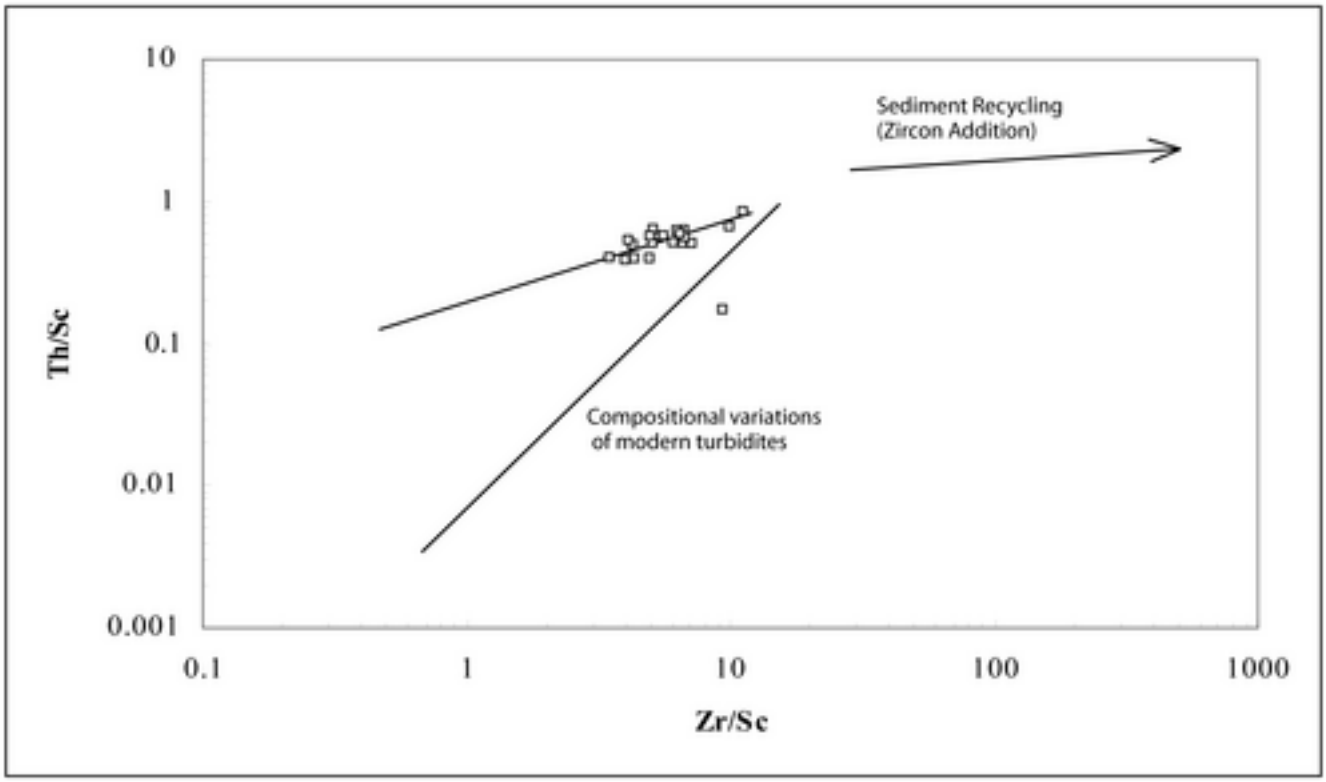
10
1
0.1
0.01
0.001
Th/Sc
0.1
1
10
100
1000
Zr/Sc
Sediment Recycling
(Zircon Addition)
Compositional variations
of modern turbidites

**Figure 11**

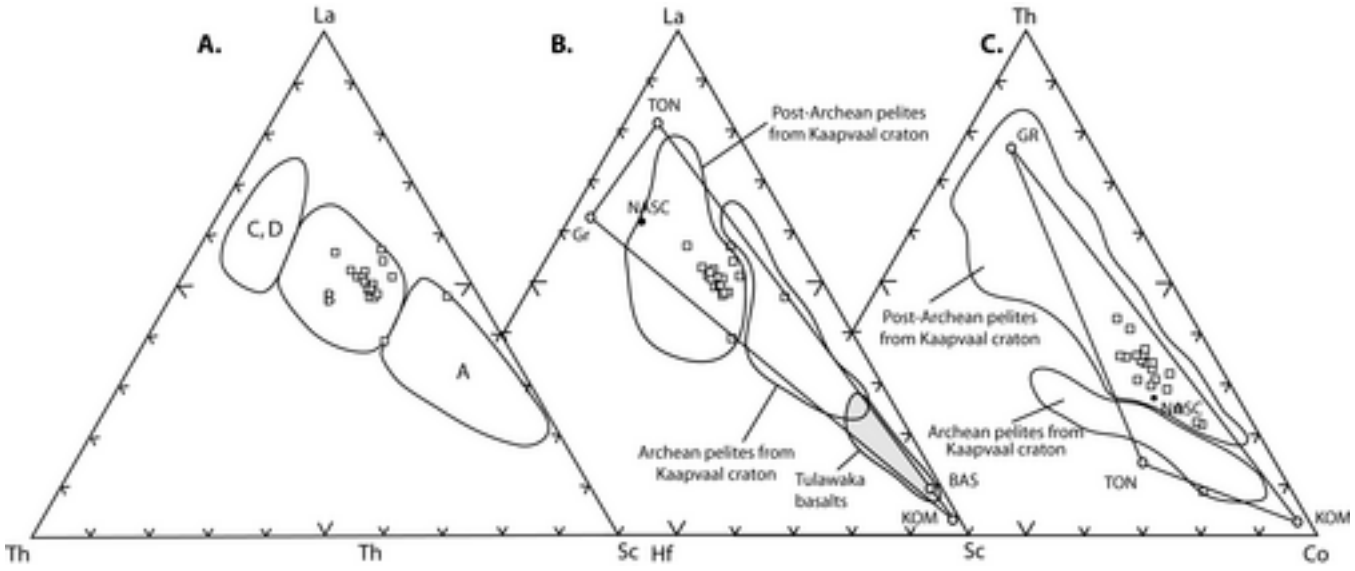
A.
La
C, D
B
A
Th
Th
B.
La
TON
Post-Archean pelites
from Kaapvaal craton
NASC
GR
Archean pelites from
Kaapvaal craton
Tulawaka
basalts
BAS
KOM
Th
Sc
Hf
C.
Th
GR
Post-Archean pelites
from Kaapvaal craton
Archean pelites from
Kaapvaal craton
TON
KOM
Sc
Co

**Figure 12**

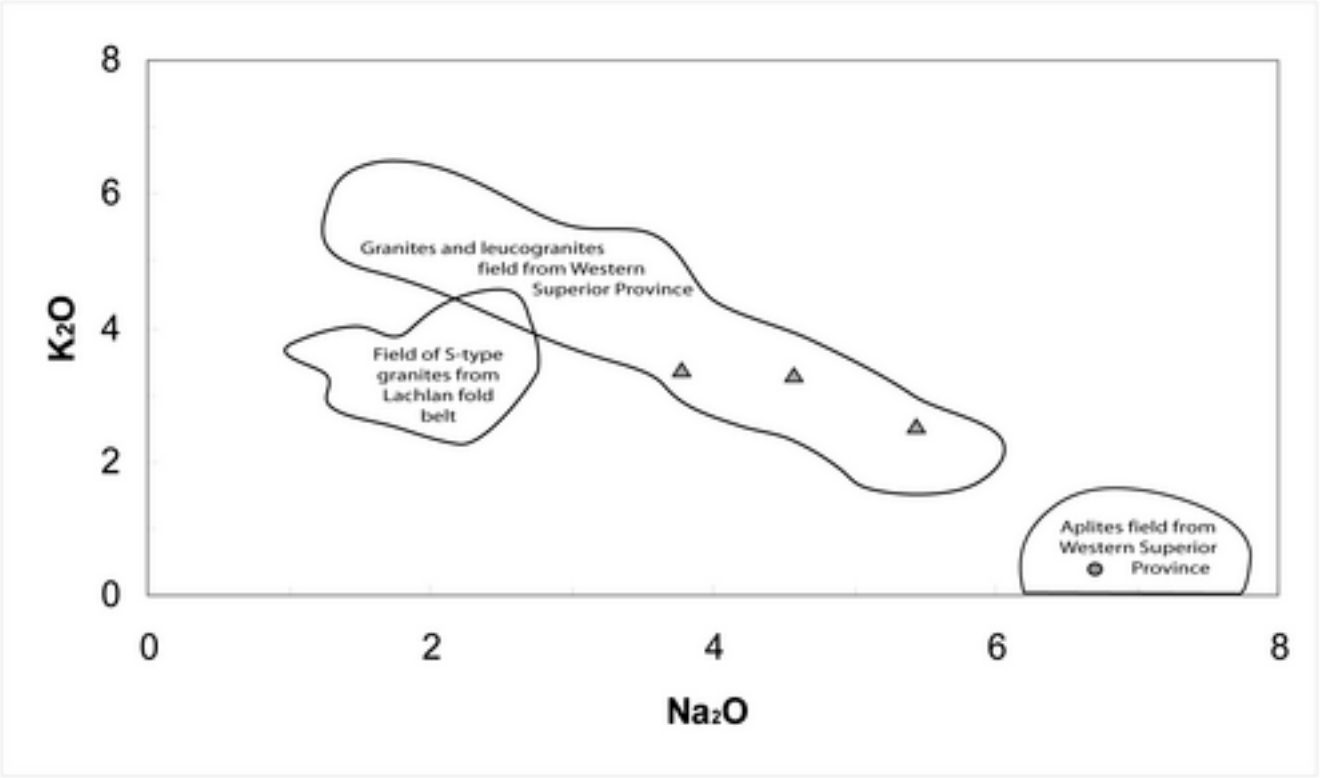
8
6
4
2
0
0
2
4
6
8
K2O
Na2O
Granites and leucogranites field from Western Superior Province
Field of S-type granites from Lachlan fold belt
Aplites field from Western Superior Province

**Figure 13**

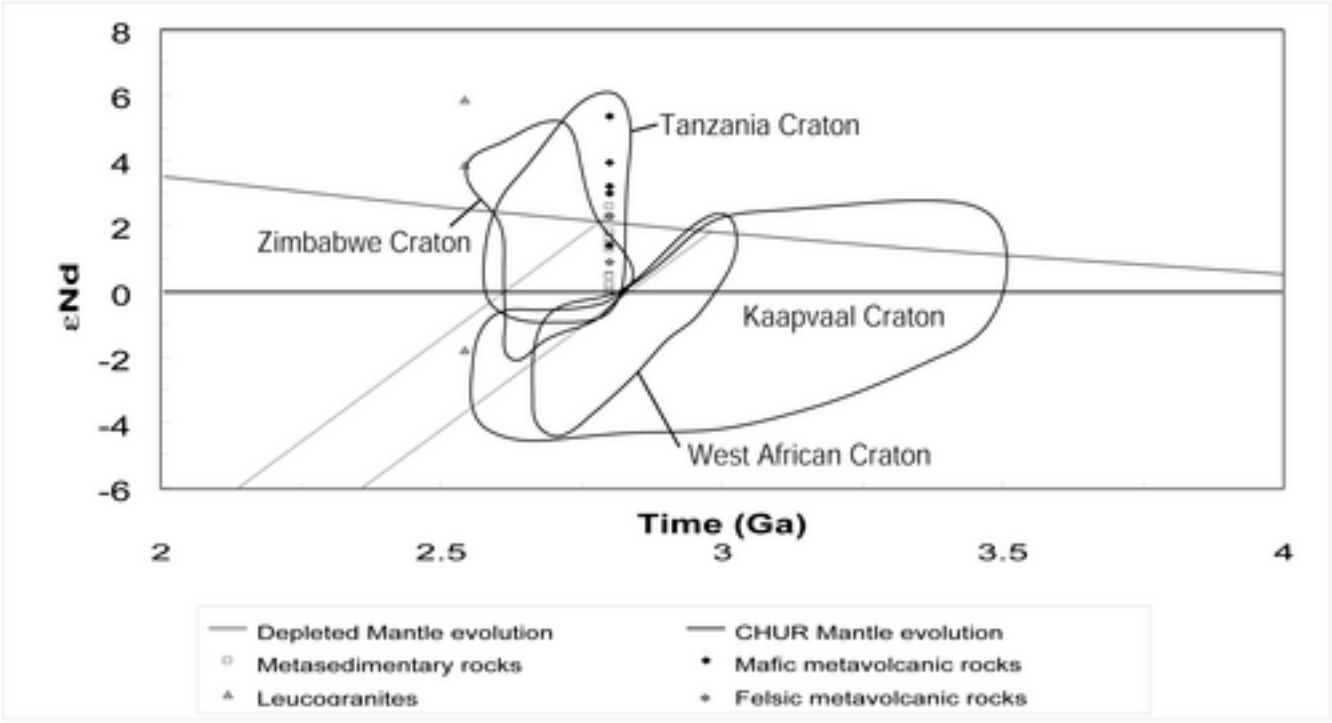
8
6
4
2
0
-2
-4
-6
εNd
Tanzania Craton
Zimbabwe Craton
Kaapvaal Craton
West African Craton
2
2.5
3
3.5
4
Time (Ga)
Depleted Mantle evolution
CHUR Mantle evolution
Metasedimentary rocks
Mafic metavolcanic rocks
Leucogranites
Felsic metavolcanic rocks

**Table 1**

| Sample | $SiO_2$ | $Al_2O_3$ | $Fe_2O_3$ | MnO | MgO | CaO | Na2O | $K_2O$ | $TiO_2$ | $P_2O_5$ | LOI | Total |
|---|---|---|---|---|---|---|---|---|---|---|---|---|
| Metasedimentary rocks : | | | | | | | | | | | | |
| D0142-1 | 64.37 | 17.82 | 4.68 | 0.062 | 2.68 | 1.04 | 2.31 | 2.56 | 0.647 | 0.11 | 2.86 | 99.15 |
| D0149-1 | 60.24 | 20.58 | 4.97 | 0.051 | 2.65 | 0.80 | 2.10 | 4.04 | 0.672 | 0.09 | 3.19 | 99.39 |
| D0149-2 | 67.61 | 14.78 | 6.00 | 0.113 | 1.77 | 3.64 | 3.37 | 0.94 | 0.546 | 0.12 | 0.74 | 99.63 |
| D0149-4 | 62.85 | 15.90 | 9.29 | 0.130 | 2.10 | 4.56 | 1.95 | 1.94 | 0.480 | 0.12 | 0.71 | 100.03 |
| D0149-6 | 53.56 | 22.81 | 7.16 | 0.056 | 3.40 | 1.03 | 1.88 | 4.51 | 0.752 | 0.10 | 4.90 | 100.18 |
| D0149-7 | 68.16 | 16.39 | 4.08 | 0.042 | 2.19 | 0.95 | 2.04 | 2.65 | 0.549 | 0.08 | 2.94 | 100.09 |
| D0149-8 | 56.91 | 23.64 | 5.73 | 0.080 | 3.11 | 0.47 | 1.32 | 4.62 | 0.722 | 0.10 | 4.21 | 100.90 |
| D0149-10 | 53.65 | 24.36 | 5.72 | 0.056 | 2.85 | 2.27 | 3.78 | 3.03 | 0.720 | 0.09 | 3.42 | 99.94 |
| D0149-12 | 61.57 | 19.99 | 7.58 | 0.054 | 2.38 | 1.09 | 1.03 | 3.85 | 0.645 | 0.10 | 2.03 | 100.32 |
| D0149-14 | 60.69 | 20.83 | 6.07 | 0.059 | 2.61 | 1.75 | 1.87 | 3.19 | 0.673 | 0.10 | 2.37 | 100.21 |
| D0149-17 | 61.68 | 20.88 | 5.06 | 0.056 | 2.52 | 1.01 | 1.47 | 3.59 | 0.663 | 0.11 | 3.22 | 100.25 |
| D0149-18 | 58.59 | 23.79 | 6.32 | 0.054 | 2.84 | 0.63 | 0.92 | 3.57 | 0.748 | 0.10 | 1.89 | 99.46 |
| D0149-19 | 57.25 | 24.33 | 6.22 | 0.047 | 2.97 | 0.50 | 0.86 | 4.28 | 0.759 | 0.10 | 2.76 | 100.07 |
| D0149-20 | 62.92 | 13.30 | 17.45 | 0.082 | 2.77 | 2.42 | 0.33 | 0.28 | 0.469 | 0.11 | 0.19 | 100.32 |
| D0159-1 | 61.22 | 19.66 | 5.77 | 0.063 | 2.99 | 1.37 | 2.93 | 2.42 | 0.695 | 0.09 | 2.90 | 100.11 |
| D0159-2 | 54.22 | 23.62 | 6.09 | 0.066 | 3.20 | 0.55 | 2.56 | 4.00 | 0.764 | 0.09 | 3.84 | 98.99 |
| D0159-3 | 61.06 | 20.59 | 6.82 | 0.042 | 2.60 | 0.87 | 1.04 | 3.96 | 0.676 | 0.12 | 2.42 | 100.19 |
| D0159-4 | 63.18 | 18.92 | 5.25 | 0.061 | 2.17 | 2.73 | 2.48 | 2.96 | 0.627 | 0.12 | 1.74 | 100.25 |
| D0159-5 | 64.19 | 19.34 | 5.20 | 0.055 | 2.30 | 1.80 | 2.37 | 2.67 | 0.631 | 0.10 | 1.60 | 100.27 |
| D0159-6 | 51.18 | 25.73 | 5.59 | 0.045 | 3.01 | 0.42 | 2.25 | 6.53 | 0.758 | 0.08 | 3.33 | 98.900 |
| D0310-2 | 54.66 | 22.91 | 6.65 | 0.042 | 2.41 | 0.40 | 0.67 | 6.28 | 0.850 | 0.13 | 5.27 | 100.27 |
| Metavolcanic rocks : | | | | | | | | | | | | |
| D0146-1 | 49.47 | 13.11 | 14.57 | 0.216 | 6.53 | 10.04 | 2.24 | 0.17 | 1.240 | 0.12 | 1.41 | 99.12 |
| D0149-3 | 57.84 | 13.87 | 14.57 | 0.169 | 2.24 | 5.94 | 0.67 | 1.38 | 0.423 | 0.14 | 1.91 | 99.15 |
| D0149-13 | 53.19 | 14.10 | 23.46 | 0.200 | 2.99 | 5.83 | 0.24 | 0.19 | 0.461 | 0.11 | -0.28 | 100.49 |
| D0185-1 | 52.55 | 12.67 | 14.73 | 0.287 | 4.71 | 6.42 | 4.50 | 0.63 | 2.206 | 0.17 | 0.66 | 99.53 |
| D0309-1 | 49.29 | 11.50 | 20.15 | 0.282 | 4.73 | 8.59 | 2.11 | 0.50 | 2.640 | 0.20 | 0.20 | 100.18 |
| D0309-2 | 51.83 | 15.16 | 13.66 | 0.161 | 3.32 | 7.11 | 3.78 | 0.43 | 1.452 | 0.24 | 2.83 | 99.96 |
| D0309-3 | 49.82 | 13.55 | 14.40 | 0.242 | 6.41 | 10.53 | 2.25 | 0.18 | 1.432 | 0.11 | 0.96 | 99.89 |
| Leucogranites : | | | | | | | | | | | | |
| D0310-1 | 75.54 | 14.32 | 1.30 | 0.254 | 0.18 | 0.43 | 3.79 | 3.35 | 0.043 | 0.03 | 1.05 | 100.29 |
| D0310-3 | 75.13 | 14.85 | 0.68 | 0.060 | 0.12 | 0.65 | 5.43 | 2.50 | 0.032 | 0.06 | 0.69 | 100.19 |
| D0310-4 | 75.82 | 14.60 | 0.67 | 0.029 | 0.10 | 0.51 | 4.58 | 3.27 | 0.027 | 0.04 | 0.71 | 100.36 |
| Aplite : | | | | | | | | | | | | |
| D0142 | 76.2 | 14.61 | 0.64 | 0.007 | 0.06 | 0.97 | 6.71 | 0.42 | 0.003 | 0.02 | 0.44 | 100.09 |

**Table 2**

| Sample | Sc | V | Cr | Co | Ni | Rb | Sr | Ba | Zr | Hf | Y | Ta | Nb | La | Ce | Pr | Nd | Sm | Eu | Gd | Tb | Dy | Ho | Er | Tm | Yb | Lu | Th | U |
|---|---|---|---|---|---|---|---|---|---|---|---|---|---|---|---|---|---|---|---|---|---|---|---|---|---|---|---|---|---|
| Metasedimentary rocks : | | | | | | | | | | | | | | | | | | | | | | | | | | | | | |
| D0142-1 | 15 | 102 | 118 | 18 | 48 | 92 | 206 | 829 | 150 | 5.2 | 14.7 | 0.69 | 7.8 | 28.4 | 55.3 | 6.36 | 23.9 | 4.26 | 1.0 | 3.29 | 0.47 | 2.58 | 0.5 | 1.56 | 0.23 | 1.5 | 0.23 | 10.3 | 3.13 |
| D0149-1 | 18 | 123 | 132 | 17 | 51 | 111 | 154 | 915 | 119 | 4.2 | 18.2 | 0.84 | 8.1 | 31.2 | 64.5 | 7.5 | 28.6 | 5.12 | 1.08 | 4.08 | 0.6 | 3.25 | 0.63 | 1.85 | 0.28 | 1.72 | 0.25 | 11.2 | 3.32 |
| D0149-2 | 9 | 82 | 78 | 14 | 29 | 32 | 389 | 328 | 84 | 2.8 | 9.5 | 0.27 | 3.2 | 9.37 | 20.3 | 2.56 | 10.9 | 2.26 | 0.76 | 2.01 | 0.31 | 1.64 | 0.31 | 0.88 | 0.12 | 0.79 | 0.11 | 1.6 | 0.47 |
| D0149-4 | 12 | 79 | 83 | 12 | 39 | 105 | 231 | 540 | 83 | 2.9 | 12.8 | 0.36 | 4.3 | 18.8 | 38.1 | 4.48 | 17.5 | 3.26 | 1.01 | 2.76 | 0.39 | 2.13 | 0.41 | 1.19 | 0.17 | 1.11 | 0.17 | 6.28 | 1.85 |
| D0149-6 | 25 | 152 | 170 | 20 | 88 | 147 | 229 | 848 | 104 | 3.8 | 18.3 | 0.73 | 7.9 | 36.3 | 76.9 | 9.21 | 36.0 | 6.64 | 1.23 | 5.06 | 0.69 | 3.46 | 0.63 | 1.85 | 0.27 | 1.71 | 0.25 | 9.67 | 3.77 |
| D0149-7 | 13 | 85 | 112 | 15 | 43 | 93 | 209 | 625 | 148 | 5.0 | 17.8 | 0.55 | 6.6 | 31.9 | 61.7 | 6.98 | 26.4 | 4.5 | 1.04 | 3.61 | 0.52 | 2.92 | 0.57 | 1.7 | 0.26 | 1.57 | 0.23 | 11.0 | 3.34 |
| D0149-8 | 23 | 142 | 158 | 19 | 64 | 153 | 186 | 951 | 115 | 4.3 | 21.4 | 0.75 | 8.4 | 37.3 | 74.9 | 8.61 | 32.7 | 5.84 | 1.17 | 4.73 | 0.71 | 3.97 | 0.76 | 2.26 | 0.34 | 2.16 | 0.32 | 13.0 | 3.44 |
| D0149-10 | 21 | 122 | 152 | 19 | 60 | 123 | 409 | 560 | 108 | 4.1 | 18.6 | 0.78 | 9.0 | 36.1 | 73.2 | 8.49 | 32.5 | 5.95 | 1.52 | 4.41 | 0.63 | 3.45 | 0.66 | 2.05 | 0.3 | 1.97 | 0.29 | 13.4 | 3.57 |
| D0149-12 | 20 | 117 | 126 | 19 | 57 | 185 | 162 | 1 240 | 114 | 4.1 | 18.8 | 0.66 | 7.7 | 30.4 | 61.1 | 7.0 | 26.9 | 4.83 | 0.87 | 3.88 | 0.58 | 3.28 | 0.64 | 1.88 | 0.29 | 1.84 | 0.27 | 11.4 | 3.21 |
| D0149-14 | 19 | 119 | 128 | 17 | 53 | 146 | 267 | 659 | 121 | 4.4 | 19.4 | 0.7 | 7.8 | 32.0 | 65.1 | 7.53 | 28.9 | 5.25 | 1.14 | 4.33 | 0.63 | 3.48 | 0.66 | 1.89 | 0.28 | 1.67 | 0.26 | 11.8 | 3.25 |
| D0149-17 | 20 | 121 | 128 | 18 | 52 | 124 | 241 | 806 | 131 | 4.4 | 20.4 | 0.67 | 7.9 | 30.6 | 61.9 | 7.28 | 27.7 | 5.18 | 1.20 | 4.2 | 0.61 | 3.44 | 0.66 | 2.08 | 0.32 | 2.0 | 0.31 | 11.8 | 3.21 |
| D0149-18 | 25 | 155 | 164 | 22 | 71 | 145 | 190 | 741 | 102 | 3.8 | 21.4 | 0.76 | 8.8 | 34.9 | 70.6 | 8.4 | 32.5 | 5.8 | 1.10 | 4.31 | 0.66 | 3.69 | 0.72 | 2.22 | 0.34 | 2.13 | 0.31 | 13.1 | 3.44 |
| D0149-19 | 25 | 155 | 168 | 24 | 75 | 142 | 242 | 790 | 105 | 3.8 | 20.5 | 0.77 | 8.4 | 34.6 | 70.6 | 8.23 | 32.0 | 5.79 | 1.29 | 4.53 | 0.68 | 3.66 | 0.69 | 2.04 | 0.3 | 1.90 | 0.28 | 12.6 | 3.37 |
| D0149-20 | 13 | 70 | 84 | 13 | 36 | 27 | 73 | 82 | 85 | 3.2 | 13.8 | 0.45 | 5.7 | 18.0 | 37.1 | 4.31 | 16.5 | 3.08 | 0.84 | 2.61 | 0.4 | 2.31 | 0.46 | 1.41 | 0.21 | 1.33 | 0.2 | 7.06 | 2.09 |
| D0159-1 | 18 | 114 | 138 | 18 | 37 | 82 | 263 | 662 | 110 | 4.0 | 14.3 | 0.77 | 8.8 | 17.5 | 36.5 | 4.29 | 16.6 | 3.22 | 0.93 | 2.74 | 0.43 | 2.43 | 0.46 | 1.41 | 0.21 | 1.36 | 0.2 | 9.5 | 3.01 |
| D0159-2 | 26 | 158 | 191 | 29 | 76 | 129 | 247 | 920 | 116 | 3.5 | 23.2 | 0.83 | 23 | 43.0 | 80.9 | 10.0 | 35.2 | 6.41 | 1.35 | 4.82 | 0.76 | 4.25 | 0.89 | 2.31 | 0.35 | 2.2 | 0.32 | 10.6 | 3.09 |
| D0159-3 | 22 | 126 | 133 | 17 | 57 | 135 | 173 | 972 | 113 | 4.2 | 19.6 | 0.97 | 8.2 | 30.6 | 61.9 | 7.28 | 28.1 | 5.04 | 0.87 | 4.04 | 0.59 | 3.27 | 0.66 | 2.05 | 0.31 | 1.96 | 0.29 | 11.5 | 3.25 |
| D0159-4 | 19 | 104 | 116 | 18 | 49 | 126 | 366 | 622 | 128 | 4.6 | 17.2 | 0.65 | 7.5 | 28.8 | 57.5 | 6.64 | 25.1 | 4.52 | 1.18 | 3.65 | 0.54 | 2.98 | 0.56 | 1.66 | 0.25 | 1.58 | 0.23 | 10.7 | 3.19 |
| D0159-5 | 18 | 107 | 126 | 15 | 104 | 119 | 279 | 653 | 117 | 42 | 17.3 | 0.66 | 7.8 | 31.1 | 61.1 | 6.82 | 25.6 | 4.45 | 1.26 | 3.72 | 0.53 | 2.92 | 0.57 | 1.76 | 0.24 | 1.55 | 0.23 | 10.5 | 2.93 |
| D0159-6 | 28 | 173 | 186 | 33 | 82 | 191 | 172 | 1 530 | 99 | 3.2 | 25.1 | 0.88 | 21.2 | 51.9 | 94.5 | 11.7 | 41.1 | 7.36 | 1.35 | 5.46 | 0.82 | 4.68 | 0.95 | 2.47 | 0.37 | 2.35 | 0.33 | 11.2 | 3.13 |
| D0310-2 | 24 | 161 | 153 | 13 | 61 | 277 | 54 | 1 050 | 116 | 4.4 | 14.6 | 0.78 | 9.1 | 20.7 | 45.3 | 5.34 | 20.8 | 4.02 | 0.77 | 3.29 | 0.45 | 2.46 | 0.48 | 1.48 | 0.23 | 1.52 | 0.24 | 9.66 | 5.24 |

bd : below detection

| Sample | Sc | V | Cr | Co | Ni | Rb | Sr | Ba | Zr | Hf | Y | Ta | Nb | La | Ce | Pr | Nd | Sm | Eu | Gd | Tb | Dy | Ho | Er | Tm | Yb | Lu | Th | U |
|---|---|---|---|---|---|---|---|---|---|---|---|---|---|---|---|---|---|---|---|---|---|---|---|---|---|---|---|---|---|
| Metavolcanic rocks : | | | | | | | | | | | | | | | | | | | | | | | | | | | | | |
| D0146-1 | 41 | 313 | 52 | 41 | 42 | 11 | 116 | 75 | 66 | 2.5 | 24.6 | 0.22 | 3.8 | 4.12 | 10.6 | 1.62 | 8.4 | 2.66 | 0.98 | 3.40 | 0.64 | 4.08 | 0.88 | 2.68 | 0.42 | 2.53 | 0.39 | 0.93 | 0.27 |
| D0149-3 | 7 | 51 | 33 | 6 | bd | 106 | 114 | 240 | 91 | 3 | 11.0 | 0.22 | 3.6 | 11.70 | 23.9 | 2.96 | 12.2 | 2.39 | 1.00 | 2.07 | 0.29 | 1.58 | 0.31 | 0.91 | 0.12 | 0.84 | 0.12 | 3.13 | 0.88 |
| D0149-13 | 14 | 76 | 71 | 9 | bd | 5 | 24 | 26 | 92 | 3.2 | 13.9 | 0.53 | 5.1 | 16.2 | 34.2 | 4.06 | 16.2 | 3.11 | 0.87 | 2.67 | 0.40 | 2.31 | 0.47 | 1.43 | 0.22 | 1.36 | 0.21 | 6.67 | 1.88 |
| D0185-1 | 52 | 454 | bd | 17 | bd | 30 | 206 | 131 | 143 | 5.2 | 45.6 | 0.41 | 6.3 | 5.05 | 13.8 | 2.18 | 12.1 | 4.35 | 1.29 | 6.14 | 1.19 | 7.47 | 1.58 | 4.79 | 0.78 | 4.65 | 0.70 | 1.55 | 0.56 |
| D0309-1 | 47 | 443 | 20 | 43 | 31 | 12 | 113 | 96 | 132 | 4.8 | 43.3 | 0.47 | 7.0 | 8.48 | 21.7 | 3.24 | 16.2 | 4.99 | 1.74 | 6.26 | 1.14 | 7.24 | 1.51 | 4.55 | 0.70 | 4.41 | 0.67 | 2.02 | 0.60 |
| D0309-2 | 30 | 224 | bd | 33 | 0 | 21 | 184 | 103 | 141 | 5 | 43.1 | 0.45 | 6.8 | 11.7 | 27.0 | 3.88 | 18.8 | 5.28 | 1.83 | 6.43 | 1.17 | 7.15 | 1.50 | 4.49 | 0.70 | 4.28 | 0.64 | 2.63 | 1.09 |
| D0309-3 | 45 | 357 | 58 | 42 | 49 | 7 | 117 | 54 | 64 | 2.4 | 24.3 | 0.21 | 3.9 | 3.98 | 10.2 | 1.56 | 8.0 | 2.56 | 1.00 | 3.33 | 0.64 | 4.01 | 0.84 | 2.57 | 0.40 | 2.44 | 0.37 | 0.88 | 0.25 |
| Leucogranites : | | | | | | | | | | | | | | | | | | | | | | | | | | | | | |
| D0310-1 | 8 | bd | 54 | bd | bd | 393 | 8 | 24 | 31 | 2.7 | 46.8 | 2.26 | 20.1 | 5.72 | 13.5 | 1.83 | 6.9 | 2.40 | 0.07 | 2.92 | 0.82 | 6.25 | 1.37 | 4.82 | 1.03 | 7.84 | 1.23 | 8.5 | 2.00 |
| D0310-3 | 4 | bd | bd | bd | bd | 290 | 7 | 10 | 40 | 3.6 | 51.0 | 5.49 | 23.3 | 10.50 | 28.5 | 3.99 | 17.0 | 6.70 | 0.05 | 6.81 | 1.37 | 7.82 | 1.43 | 4.36 | 0.76 | 4.90 | 0.73 | 16.9 | 8.51 |
| D0310-4 | 5 | bd | bd | bd | bd | 350 | 7 | 13 | 30 | 3 | 40.9 | 5.52 | 25 | 10.70 | 27.5 | 3.77 | 15.5 | 5.31 | 0.03 | 5.51 | 1.06 | 6.31 | 1.19 | 3.68 | 0.66 | 4.17 | 0.62 | 12.9 | 15.10 |
| Aplite : | | | | | | | | | | | | | | | | | | | | | | | | | | | | | |
| D0142 | 2 | bd | bd | bd | bd | 19 | 148 | 35 | 37 | 3.5 | 1.7 | 1.84 | 13.1 | 1.48 | 4.00 | 0.63 | 3.3 | 2.29 | 0.15 | 2.30 | 0.26 | 0.63 | 0.04 | 0.06 | bd | 0.04 | bd | 9.01 | 16.80 |

bd : below detection

**Table 3**

| Sample | Rock type | Age (Ga) | Sm(ppm)[a] | Nd (ppm)[a] | $^{147}Sm/^{144}Nd$[a] | $^{143}Nd/^{144}Nd$ (± 2σ) | εNd(t)[b] | $T_{dm}$[c] |
|---|---|---|---|---|---|---|---|---|
| D0142-1 | S | 2.8 | 4.57 | 26.9 | 0.1025 | 0.510950 ± 0.000010 | 1.0 | 3.00 |
| D0142-2 | S | 2.8 | 6.28 | 36.3 | 0.1044 | 0.511004 ± 0.000013 | 1.3 | 2.98 |
| D0149-1 | S | 2.8 | 5.76 | 32.0 | 0.1055 | 0.510977 ± 0.000015 | 0.5 | 3.04 |
| D0149-2 | S | 2.8 | 2.65 | 13.3 | 0.1204 | 0.511360 ± 0.000013 | 2.6 | 2.91 |
| D0149-4 | S | 2.8 | 3.80 | 21.1 | 0.1090 | 0.511132 ± 0.000010 | 2.3 | 2.92 |
| D0149-5 | S | 2.8 | 3.70 | 21.3 | 0.1052 | 0.510958 ± 0.000010 | 0.2 | 3.06 |
| D0149-7 | S | 2.8 | 5.49 | 33.1 | 0.1003 | 0.510939 ± 0.000010 | 1.6 | 2.95 |
| D0149-8 | S | 2.8 | 6.31 | 36.4 | 0.1047 | 0.510939 ± 0.000010 | 0.0 | 3.07 |
| D0149-20 | S | 2.8 | 3.66 | 20.4 | 0.1084 | 0.511080 ± 0.000010 | 1.5 | 2.98 |
| D0159-1 | S | 2.8 | 3.33 | 18.3 | 0.1098 | 0.511055 ± 0.000011 | 0.4 | 3.06 |
| D0159-2 | S | 2.8 | 6.88 | 38.8 | 0.1072 | 0.511061 ± 0.000010 | 1.5 | 2.97 |
| D0159-3 | S | 2.8 | 5.80 | 33.3 | 0.1055 | 0.511045 ± 0.000010 | 1.8 | 2.95 |
| D0159-4 | S | 2.8 | 5.22 | 30.4 | 0.1036 | 0.510989 ± 0.000010 | 1.4 | 2.98 |
| D0159-5 | S | 2.8 | 4.99 | 29.7 | 0.1015 | 0.510961 ± 0.000010 | 1.6 | 2.96 |
| D0159-6 | S | 2.8 | 6.84 | 39.2 | 0.1053 | 0.511028 ± 0.000010 | 1.6 | 2.97 |
| D0310-2 | S | 2.8 | 4.64 | 25.3 | 0.1107 | 0.511047 ± 0.000014 | 0.0 | 3.10 |
| D0146-1 | V | 2.8 | 3.91 | 12.9 | 0.1826 | 0.512528 ± 0.000010 | 3.2 | |
| D0149-3 | V | 2.8 | 2.77 | 14.6 | 0.1144 | 0.511235 ± 0.000010 | 2.3 | 2.93 |
| D0149-13 | V | 2.8 | 3.68 | 19.9 | 0.1121 | 0.511119 ± 0.000010 | 0.9 | 3.03 |
| D0185-1 | V | 2.8 | 4.75 | 13.6 | 0.2120 | 0.512992 ± 0.000009 | 1.4 | |
| D0309-1 | V | 2.8 | 5.44 | 18.6 | 0.1767 | 0.512469 ± 0.000010 | 3.9 | |
| D0309-2 | V | 2.8 | 6.03 | 22.5 | 0.1622 | 0.512272 ± 0.000010 | 5.3 | |
| D0309-3 | V | 2.8 | 2.83 | 9.3 | 0.1841 | 0.512557 ± 0.000010 | 3.0 | |
| D0310-1 | L | 2.5 | 2.67 | 8.1 | 0.1990 | 0.512878 ± 0.000010 | 3.9 | |
| D0310-3 | L | 2.5 | 7.52 | 20.2 | 0.2251 | 0.513072 ± 0.000010 | -0.7 | |
| D0310-4 | L | 2.5 | 5.98 | 18.5 | 0.1956 | 0.512916 ± 0.000010 | 5.8 | |
| D0149-4 (S) | G | 2.8 | 2.72 | 11.7 | 0.1408 | 0.511747 ± 0.000010 | 2.8 | 2.92 |
| D0149-13 (V) | G | 2.8 | 3.18 | 15.3 | 0.1258 | 0.511360 ± 0.000010 | 0.6 | 3.09 |
| D0149-20 (S) | G | 2.8 | 2.77 | 10.0 | 0.1526 | 0.511749 ± 0.000010 | -1.5 | |
| D0149-20 (S)[d] | G | 2.8 | 2.85 | 10.6 | 0.1622 | 0.511831 ± 0.000010 | -3.3 | |
| D0310-1 (L) | G | 2.5 | 9.49 | 12.4 | 0.4617 | 0.517284 ± 0.000010 | 5.5 | |
| D0142 | A | 2.5 | 2.92 | 4.4 | 0.4015 | 0.515373 ± 0.000010 | -12.6 | |

a. Sm, Nd concentration and Sm/Nd ratios have an accuracy of 0.5%.

b. Error on εNd is ± 0.5 unit .

c. Depleted mantle model ages (DePaolo, 1981)

d. Finer grained garnet fraction

S = Metasedimentary, V = Metavolcanic, L = Leucogranite and G = Garnet